

JPET #198770

**Identification and functional characterization of a novel UGT2A1 splice variant:  
Potential importance in tobacco-related cancer susceptibility\***

Ryan T. Bushey and Philip Lazarus

Departments of Pharmacology (R.T.B. and P.L.) and Public Health Sciences (P.L.),  
Penn State University College of Medicine, 500 University Drive, Hershey, PA, 17033,  
USA

JPET #198770

**Running title:** Characterization of the UGT2A1 exon 3 splice variant

**Corresponding author:** Philip Lazarus, Ph.D., Department of Pharmacology, Penn State University College of Medicine, Mail Code-CH69, 500 University Drive, Hershey PA, 17033; Phone: 717-531-5734; Fax: (717)-531-0480;  
Email: [plazarus@psu.edu](mailto:plazarus@psu.edu)

**Document Statistics:**

Text pages: 52

Tables: 1

Figures: 6

References: 46

Abstract words: 244

Introduction words: 703

Discussion words: 1103

**Abbreviations:** UDP-Glucuronosyltransferase (UGT); polycyclic aromatic hydrocarbon (PAH); Ponasterone A (PonA); reverse-transcription polymerase chain reaction (RT-PCR); co-immunoprecipitation (co-IP); ultra-pressure liquid chromatography (UPLC)

**Recommended section:** Metabolism, Transport, and Pharmacogenomics

JPET #198770

## Abstract

UGT2A1 is a respiratory and aerodigestive tract-expressing phase II detoxifying enzyme that metabolizes various xenobiotics including polycyclic aromatic hydrocarbons (PAHs). In the present study, a novel exon 3 deletion splice variant was identified for UGT2A1 (termed 'UGT2A1 $\Delta$ exon3'). As determined by reverse-transcription polymerase chain reaction, UGT2A1 $\Delta$ exon3 was shown to be expressed in various tissues including lung, trachea, larynx, tonsil, and colon. The ratio of UGT2A1 $\Delta$ exon3:wild-type UGT2A1 expression was highest in colon (0.79 $\pm$ 0.08) and lung (0.42 $\pm$ 0.12) as determined by real-time PCR; an antibody specific to UGT2A1 showed splice variant protein (termed 'UGT2A1\_i2') to wild-type protein (termed 'UGT2A1\_i1') ratios in the range of 0.5-0.9 in these tissues. Using ultra-pressure liquid chromatography, homogenates prepared from UGT2A1\_i2-over-expressing HEK293 cells exhibited no glucuronidation activity against PAHs, including benzo(a)pyrene-7,8-dihydrodiol (B(a)P-7,8-diol). An inducible *in vitro* system was created to determine the effect of UGT2A1\_i2 expression on UGT2A1\_i1 activity. Increasing UGT2A1\_i2 levels resulted in a significant ( $p < 0.01$ ) decrease in the UGT2A1\_i1  $V_{max}$  against 1-hydroxy (OH)-pyrene, 3-OH-B(a)P and B(a)P-7,8-diol; no significant changes in  $K_M$  were observed for any of the three substrates. Co-immunoprecipitation experiments suggested the formation of UGT2A1\_i1 and UGT2A1\_i2 hetero-oligomers and UGT2A1\_i1 homo-oligomers; co-expression of UGT2A1\_i1 or UGT2A1\_i2 with other UGT1A or UGT2B enzymes caused no change in UGT1A or UGT2B glucuronidation activity. These data suggest that a novel UGT2A1 splice variant regulates UGT2A1-

JPET #198770

mediated glucuronidation activity via UGT2A1-specific protein-protein interactions, and that expression of this variant could play an important role in the detoxification of carcinogens within target tissues for tobacco carcinogenesis.

## Introduction

The UDP-Glucuronosyltransferase (UGT) family of enzymes catalyzes the metabolism of various xenobiotics, including endogenous substrates such as steroid hormones and exogenous substrates such as various drugs and carcinogens (Wells et al., 2004; Nagar and Rimmel, 2006). UGT enzymes are classified into families based on sequence and structural homology (Mackenzie et al., 2005). Enzymes in the UGT1A and UGT2B families are the most well-known and studied UGTs, with nine functional UGT1A isoforms and seven functional UGT2B isoforms previously characterized (Mackenzie et al., 2005). In comparison to the UGT1A and UGT2B enzyme families, the UGT2A family has been relatively understudied. Recent evidence suggests that one member of the UGT2A subfamily, UGT2A1, may be an important enzyme for tobacco carcinogen metabolism in respiratory and aerodigestive tract tissues (Bushey et al., 2011).

UGT2A1 was initially cloned from the olfactory epithelium, with enzyme expression also reported in fetal lung and brain (Jedlitschky et al., 1999). A later study reported UGT2A1 expression in lung and trachea by quantitative real-time polymerase chain reaction (PCR) (Nishimura and Naito, 2006). More recent quantitative PCR studies have shown UGT2A1 expression to be highest in lung followed by trachea, tonsil, larynx, and colon (Bushey et al., 2011). UGT2A1 enzymatic activity was initially reported against substrates such as androgens, estrogens, drugs, and phenol odorants (Jedlitschky et al., 1999; Itaaho et al., 2008; Sten et al., 2009). Recent studies have

JPET #198770

shown significant UGT2A1 enzyme activity against polycyclic aromatic hydrocarbons (PAHs) implicated in lung and aerodigestive tract carcinogenesis (Bushey et al., 2011). While other UGTs such as UGT1A6, UGT1A7, and UGT1A10 have been reported to exhibit some activity against certain PAHs, UGT2A1 is the only UGT well-expressed in both the respiratory and aerodigestive tracts that exhibits significant glucuronidation activity against a broad range of PAHs and their metabolites (Jin et al., 1993; Zheng et al., 2002; Dellinger et al., 2006; Nishimura and Naito, 2006; Bushey et al., 2011). Based on the expression and activity profile of UGT2A1, this understudied enzyme potentially has a crucial role in the local detoxification of activated PAHs in tobacco target tissues.

Through the process of alternative splicing, single genes can produce multiple mRNA and protein isoforms with varying function. Alternative splicing was initially proposed to affect half of all genes, but recent reports suggest that alternative splicing may occur in over 90% of all genes (Lander et al., 2001; Wang et al., 2008). Recent reports suggest that alternative splicing creates UGT1A diversity at the 3' end of the transcript, through alternative splicing of a novel exon 5b (Girard et al., 2007; Levesque et al., 2007). The mRNAs resulting from alternative splicing of exon 5b have been shown to have widespread tissue expression, and functional assays have suggested that the proteins resulting from exon 5b splice variants are inactive (Girard et al., 2007). Proteins resulting from UGT1A exon 5b splice variants have also been shown to interact with UGT1A wild-type proteins and negatively modulate wild type UGT1A glucuronidation activity through a protein-protein interaction (Girard et al., 2007; Levesque et al., 2007; Bellemare et al., 2010). While UGT2B enzymes are comprised of six independent exons, alternative splicing has also been described for UGTs 2B4 and

JPET #198770

2B7, resulting in various non-functional alternatively-spliced UGT2B4 (Levesque et al., 2010) or UGT2B7 (Menard et al., 2011) variants. These splice variants have also been found to be well-expressed in various tissues, and the resulting splice variant proteins of UGT2B4 and UGT2B7 have been shown to negatively regulate wild-type UGT 2B4 and 2B7 glucuronidation activity (Levesque et al.; Menard et al.).

Similar to the UGT1A locus, diversity in the UGT2A family is created through exon sharing. UGT2A1 and UGT2A2 transcripts are comprised of a unique first exon joined to common exons 2-6 (Mackenzie et al., 2005; Sneitz et al., 2009). Unique first exons in UGT2A1 and UGT2A2 transcripts create variable aglycone-binding domains, altering the substrate specificity for each UGT isoform (Nagar and Rummel, 2006). In the present study, a novel exon 3 deletion splice variant is described for UGT2A1. This variant was hypothesized to negatively regulate UGT2A1 activity, as has been reported for other UGT splice variants. Described are studies examining the expression and function of this variant (termed 'UGT2A1 $\Delta$ exon3') and its potential importance in altering overall UGT2A1 glucuronidation activity.

## Materials and Methods

Materials. Uridine 5'-diphospho-glucuronic acid (UDPGA), alamethicin,  $\beta$ -glucuronidase, 4-methylumbelliferone (4-MU), 1-hydroxy (OH)-pyrene, and 1-naphthol were purchased from Sigma-Aldrich (St. Louis, MO). 1-OH-benzo(a)pyrene [B(a)P], 3-OH-B(a)P, 7-OH-B(a)P, 8-OH-B(a)P, 5-methyl-chrysene-1,2-diol, dibenzo(a,h)pyrene-11,12-diol, and B(a)P-7,8-diol were synthesized in the Organic Synthesis Core Facility at the Penn State College of Medicine (Hershey, PA). High-pressure liquid chromatography (HPLC)-grade ammonium acetate, acetonitrile, and agarose were purchased from Fisher Scientific (Pittsburgh, PA). Real-time PCR probes and gene expression assays were acquired from Applied Biosystems Inc., Life Technologies (Carlsbad, CA). Complete Control Inducible Mammalian Expression System kits, Ponasterone A (PonA), and *Pfu* Polymerase were obtained from Agilent (Santa Clara, CA). Dulbecco's modified Eagles medium (DMEM), Dulbecco's phosphate-buffered saline (minus calcium-chloride and magnesium-chloride), fetal bovine serum (FBS), penicillin-streptomycin, geneticin (G418), and blasticidin were purchased from Gibco, Life Technologies (Grand Island, NY). The pcDNA 3.1/V5-His-TOPO and pcDNA6.2/V5/GW/D-TOPO mammalian expression vectors, the Superscript II RT kit, and Hygromycin B were obtained from Invitrogen, Life Technologies (Grand Island, NY). The BCA protein assay kit was purchased from Pierce (Rockford, IL). The RNeasy kit, QIAquick gel extraction kit, Plasmid Mini kit, and Plasmid Maxi kit were all purchased



JPET #198770

from Qiagen (Valencia, CA). All oligonucleotides were purchased from IDT (Coralville, IA).

Determination of UGT2A1 $\Delta$ exon3 tissue expression. The UGT2A1 exon 3 deletion splice variant was initially discovered following reverse-transcription (RT)-PCR using pooled lung RNA from three individuals. The primers used to amplify full length UGT2A1 $\Delta$ exon3 from lung cDNA were 5'-CATCAAATCTTCTGCATCAAGCCAC-3' (sense; UGT2A1\_S1) and 5'-TGACAGGAAGAGGGTATAGTCAGC-3' (antisense; UGT2A1\_AS1), corresponding to nucleotides -28 to -4 and +1834 to +1811, respectively, relative to the UGT2A1 translation start site. For all PCR reactions, RNA was acquired and RT-PCR was completed as previously described (Bushey et al., 2011). Briefly, 2  $\mu$ g of RNA from each tissue was used with oligo dTs for RT, with cDNA corresponding to 100 ng of RNA used in the subsequent PCR reactions. Unless otherwise noted, all PCRs were performed using *Pfu* Polymerase, with an initial denaturing temperature of 94°C for 2 min, 40 cycles of 94°C for 30s, 58°C for 45s, and 72°C for 2 min, followed by a final cycle of 10 min at 72°C.

Following the initial discovery of UGT2A1 $\Delta$ exon 3 from pooled lung cDNA, additional tissues were screened for UGT2A1 $\Delta$ exon3 mRNA expression by RT-PCR and real-time PCR using pooled RNAs from at least three individuals. Primers specific to exon 1 5'-GACATGGCTGGAAAATAGACC-3' (sense) and exon 5 of UGT2A1 5'-CCATAGGGACTCCGTGGTAAAT-3' (antisense) of UGT2A1, corresponding to nucleotides +276 to +296 and +1165 to +1144, respectively, relative to the translation start site were used to screen for UGT2A1 $\Delta$ exon3 expression. RT was completed using

JPET #198770

RNAs from HEK293 cell lines over-expressing wild-type UGT2A1 or UGT2A1 $\Delta$ exon3 (see below for Methods), and cDNAs following RT were used as positive controls for PCR amplification while water was used as a negative control. PCR products were gel-purified using a QIAquick gel extraction kit and sequenced by dideoxy sequencing at the Penn State University Nucleic Acid Facility (State College, PA) and compared to the UGT2A1 sequence in GenBank (NM\_006798.3). To verify UGT2A1 $\Delta$ exon3 expression in tissues analyzed, PCR reactions were run multiple times with all positive and negative controls. Genomic DNA from five individuals was PCR amplified to determine whether prevalent splice site polymorphisms exist in introns 2 or 3 of UGT2A1. A sense primer specific for the 3' end of UGT2A1 exon 2 and an anti-sense primer specific for UGT2A1 exon 3 were used to amplify intron 2, while a sense primer specific for exon 3 and an anti-sense primer specific for the 5' end of UGT2A1 exon 4 were used to amplify intron 3. Following PCR amplification the PCR products were gel extracted and sequenced.

A real-time PCR assay was developed to quantitatively assess relative levels of wild-type UGT2A1 and UGT2A1 $\Delta$ exon3 transcripts in tissues that were previously determined to have UGT2A1 expression. Separate assays were designed to specifically amplify wild-type UGT2A1 or UGT2A1 $\Delta$ exon3 (see Figure 1, Panel A). A sense primer specific to exon 1 (5'-CTACATGTTTGAAACTCTTTGGAAATC-3') and a 5' labeled VIC probe (ABI) specific to exon 2 (5'-TCCGAACATATTGGGATT-3'), corresponding to nucleotides +660 to +686 and +767 to +784, respectively, relative to the UGT2A1 translation start site, were used to detect both wild-type UGT2A1 and UGT2A1 $\Delta$ exon3. An antisense primer specific to UGT2A1 exon 3 (5'-TTACCTGAGCTCTGGAT-

JPET #198770

AAATTCTTC-3'), corresponding to nucleotides +896 to +871 relative to the UGT2A1 translation start site, was used to specifically amplify wild-type UGT2A1 transcript, while an antisense primer specific to the UGT2A1 $\Delta$ exon3 exon 2 and 4 junction (5'-TTTCCTTTGTATCTCCATAAAACCTTAG-3'), corresponding to nucleotides +887 to +860 relative to the UGT2A1 $\Delta$ exon3 translation start site, was used to specifically amplify the UGT2A $\Delta$ exon3 transcript. Reactions were completed using the standard ABI thermal cycling parameters, with human large ribosomal protein (RPLPO; Hs99999902\_m1) used as a housekeeping gene. cDNAs, corresponding to 20 ng RNA, were used for each real-time assay and reactions were performed in triplicate. Real-time PCR experiments were carried out in the Penn State College of Medicine Functional Genomics Core Facility (Hershey, PA) using an ABI 7900 HT thermal cycler and data was analyzed using SDS 2.2 software. Assay specificity for wild-type UGT2A1 or UGT2A1 $\Delta$ exon3 transcripts was confirmed through agarose gel electrophoresis and dideoxy sequencing of real-time PCR products. Real-time PCR data was corrected to account for the amplification efficiency of each real-time PCR assay, as described previously (Jones et al., 2012). The relative tissue expression of UGT2A1 $\Delta$ exon3 transcript was calculated using the  $\Delta\Delta$ Ct method relative to the amount of wild-type UGT2A1 transcript for each tissue specimen examined.

*Generation of an UGT2A1 i2 over-expressing cell line and determination of UGT2A1 i2 protein expression.* A HEK293 cell line over-expressing wild-type UGT2A1 (termed 'UGT2A1\_i1') was previously established (Bushey et al., 2011). A HEK293 cell line over-expressing the isoform corresponding to UGT2A1exon $\Delta$ 3 (termed

JPET #198770

'UGT2A1\_i2') was created and cell homogenates were made using a similar protocol (described in Supplemental Methods). An antibody designed to recognize UGT2A1 protein was previously created using a peptide encoded by exon 1, a region common to both UGT2A1\_i1 and UGT2A1\_i2 (Bushey et al., 2011). Levels of UGT2A1\_i1 and UGT2A1\_i2 protein were determined by Western blot analysis using the anti-UGT2A1 antibody at a 1:500 dilution (as recommended by the manufacturer; Open Biosystems, Huntsville, AL) and 50  $\mu$ g of UGT2A1-over-expressing cell homogenate protein. The monoclonal  $\beta$ -actin antibody (Sigma-Aldrich; St. Louis, MO) was used as a loading control and the Western blot was done in triplicate. The intensity of UGT2A1 signal was measured with the ImageJ program (NIH). Since a UGT2A1 standard is not commercially available, the relative protein expression of UGT2A1\_i1 and UGT2A1\_i2 in homogenate from each cell line was calculated relative to the  $\beta$ -actin loading control. UGT2A1 protein expression was also analyzed in normal human lung and colon homogenates prepared from tissues from independent subjects (obtained from Banner Sun Health Research Institute, Sun City, AZ) by a similar Western blot procedure, using 250  $\mu$ g tissue homogenate prepared using an Omni TH rotor-stator homogenizer in 50 mM Tris pH 7.5, 1.15% KCl, and 1 mM disodium EDTA. For the determination of UGT2A1 expression in colon and lung tissue homogenates, protein from cell lines over-expressing UGT2A1\_i1 and UGT2A1\_i2 was mixed in a 1:1 ratio and loaded (60  $\mu$ g total protein) as a positive control. The relative amount of UGT2A1\_i2 to UGT2A1\_i1 in each lung or colon specimen was determined relative to  $\beta$ -actin as described above.

JPET #198770

Glucuronidation assays. Glucuronidation assays using homogenate from HEK293 cells over-expressing UGT2A1\_i1 and UGT2A1\_i2 were completed essentially as previously described (Fang et al., 2002; Wiener et al., 2004a). Briefly, after an initial incubation of 100 µg protein homogenate with alamethicin (50 µg/mg protein) for 15 minutes on ice, glucuronidation reactions were performed in a final reaction volume of 25 µL at 37°C with 50 mM Tris-HCl (pH 7.4), 10 mM MgCl<sub>2</sub>, 4 mM UDPGA, and between 6 and 800 µM of substrate. Reactions were terminated by the addition of 25 µL cold acetonitrile on ice. Reaction mixtures were centrifuged for 10 min at 16,100 g prior to the collection of supernatant. Glucuronide formation was determined using a Waters Acquity ultra-pressure liquid chromatography (UPLC) System (Milford, MA) as previously described (Fang et al., 2002; Wiener et al., 2004b; Dellinger et al., 2007; Balliet et al., 2009; Olson et al., 2009; Bushey et al., 2011). The flow rate was maintained at 0.5 mL/min and a reverse phase Acquity UPLC BEH C18 - 1.7 µm 2.1 x 100 mm column was used to separate free substrate and the conjugated glucuronide. A gradient of solution A (5 mM NH<sub>4</sub>OAc pH 5.0, 10% acetonitrile) and solution B (100% acetonitrile) was used to elute the glucuronide and substrate from the column. The initial solvent gradients and UV absorbance wavelengths used to detect glucuronidation of various substrates were described previously (Bushey et al., 2011). Reactions with non-transfected HEK293 cell homogenate, no substrate added to the reaction mixture, or only substrate and no homogenate added to the reaction mixture were used as negative controls. Homogenate from a HEK293 cell line over-expressing UGT2A1\_i1 was used as a positive control.

JPET #198770

Creation of an UGT2A1 i2 inducible system. Wild-type UGT2A1 was cloned into the V5-tagged, blasticidin resistance gene-containing pcDNA6.2/V5/GW/D-TOPO vector using a sense primer 5'-CACCATGTTAAACAACCTTCTGC-3' (UGT2A1\_S2) and antisense primer 5'-TTCTCTTTTTTCTTCTTTCCTATCTTACC-3' (UGT2A1\_AS2) corresponding to nucleotides +1 to +19 and +1581 to +1552, respectively, relative to the UGT2A1 translation start site, amplifying the entire coding region of wild-type UGT2A1 minus the stop codon (underlined nucleotides in sense primer indicate a CACC anchor). An ecdysone-analog inducible mammalian expression system was used to regulate UGT2A1\_i2 levels, with UGT2A1 $\Delta$ exon3 cloned into the FLAG-tagged, hygromycin resistance gene-containing pEGSH vector using a similar sense primer to that described above but containing a Xho I restriction site (underlined) on the 5' end (5'-GCACTCGAGATGTTAAACAACCTTCTGC-3'; UGT2A1\_S3), and a similar antisense primer to that described above with a Xba I restriction site (underlined) on the 5' end (5'-GATTCTAGACGTTCTCTTTTTTCTTCTTTCCTATCTTACC-3'; UGT2A1\_AS3). After plasmid preparations for each clone, vector sequences were verified by direct dideoxy sequencing. Eight micrograms each of the pEGSH\_UGT2A1 $\Delta$ exon3 vector and the G418 resistance gene-containing pERV regulatory vector, comprising the inducible system, as well as the pcDNA6.2/V5/GW/D-TOPO\_wtUGT2A1 vector, were stably transfected simultaneously into HEK293 cells using a standard lipofectamine protocol. Selection of HEK293 cells over-expressing the three vectors was completed using a combination of 400  $\mu$ g/mL G418, 9  $\mu$ g/mL blasticidin, and 75  $\mu$ g/mL hygromycin B in DMEM containing 10% FBS. Multiple clones were analyzed for inducible gene expression, and a stable clone over-expressing all

JPET #198770

three vectors simultaneously was chosen based on the efficiency of UGT2A1\_i2 induction.

After the creation of the stable UGT2A1\_i1\_V5/UGT2A1\_i2\_FLAG/pERV-over-expressing cell line, UGT2A1\_i2 expression was induced with varying levels of the ecdysone-analog PonA. HEK293 cells at 50% confluence were treated with 2  $\mu$ M, 6  $\mu$ M, or 10  $\mu$ M of PonA in ethanol for 12 h. Vehicle (0.01% ethanol) was added to these cells as a negative control. Cells were harvested and homogenates were made as previously described (Dellinger et al., 2006; Sun et al., 2006). Protein homogenates from the various treatment groups were screened for UGT2A1\_i1\_V5 and UGT2A1\_i2\_FLAG expression by Western blot analysis using 50  $\mu$ g of total protein per sample, with the analysis of UGT2A1\_i2\_FLAG induction performed in triplicate. UGT2A1\_i1\_V5 expression was determined using a monoclonal mouse V5-HRP antibody (Invitrogen; Grand Island, NY) at a 1:5000 dilution, while UGT2A1\_i2\_FLAG was determined using a monoclonal mouse anti-Flag antibody (Sigma-Aldrich; St. Louis, MO) at a 1:1000 dilution. UGT2A1\_i1\_V5 and UGT2A1\_i2\_FLAG expression levels were also confirmed using the anti-UGT2A1 antibody described above, with 100  $\mu$ g of protein homogenate from both the control and 10  $\mu$ M PonA treatment groups used with the anti-UGT2A1 antibody at a 1:500 dilution. In all cases, the monoclonal  $\beta$ -actin antibody was used as a loading control.

Following verification of UGT2A1\_i1 and UGT2A1\_i2 protein levels, homogenate was prepared and used for activity assays as previously described (Dellinger et al., 2007; Sun et al., 2007; Balliet et al., 2009; Olson et al., 2009; Balliet et al., 2010; Bushey et al., 2011). Cell lysates were homogenized for 10 sec on ice using a Bio-

JPET #198770

Vortexer (Biospec Products, Bartlesville, OK). Activity was determined against three PAHs which were previously shown to be substrates of UGT2A1 (Bushey et al., 2011). Activity assays were completed in triplicate for each substrate examined, using the control cell line and cell lines treated with 2  $\mu$ M, 6  $\mu$ M, or 10  $\mu$ M of PonA. For each substrate, the glucuronidation rate was determined at 8 concentrations that encompassed the  $K_M$  of the substrate. For glucuronidation rate determinations, cell homogenate protein levels and incubation times for each substrate were determined experimentally to ensure that substrate utilization was less than 10% and to maximize the levels of detection while in a linear range of glucuronide formation. Cell lines over-expressing either UGT2A1\_i1\_V5 or UGT2A1\_i2\_FLAG alone were also created using an identical protocol for non-tagged UGT2A1\_i1 and UGT2A1\_i2-over-expressing cell lines, with cell homogenates prepared as described above.

UGT2A1\_i1 and UGT2A1\_i2 co-immunoprecipitation (IP) assays. HEK293 cells over-expressing UGT2A1\_i1\_V5/UGT2A1\_i2\_FLAG were treated with 10  $\mu$ M PonA for 12 h prior to washing with phosphate-buffered saline (PBS) and homogenate preparation as described previously (Bellemare et al., 2010). A Dynabead Protein G Immunoprecipitation Kit (Invitrogen; Grand Island, NY) using the standard protocol was used to determine potential protein interactions. Three  $\mu$ g of a mouse monoclonal anti-FLAG antibody or 1.5  $\mu$ g of mouse monoclonal V5 antibody (Santa Cruz Biotechnology; Santa Cruz, CA) were incubated with Dynabeads for 15 min with rotation at room temperature. Protein lysates at a concentration of 2.5  $\mu$ g/ $\mu$ L (1250  $\mu$ g total protein) from vehicle- or PonA-treated UGT2A1\_i1\_V5/UGT2A1\_i2\_FLAG inducible cells were then



JPET #198770

incubated with the same Dynabeads for 30 min with rotation at room temperature. Following three washes in PBS at room temperature, immunoprecipitated proteins were eluted with the provided elution buffer (Invitrogen) under denaturing conditions, heated at 90°C for 10 min in loading buffer, and subjected to Western blot analysis using either a monoclonal mouse V5-HRP antibody at a 1:5000 dilution or a mouse FLAG-HRP antibody (Cell Signaling Technology; Beverly, MA) at a 1:1000 dilution. All co-IP experiments were repeated 4x. UGT2A1\_i1 homo-oligomerization was investigated using a similar protocol (described in the Supplemental Methods).

*Co-expression of UGT2A1\_i1 and UGT2A1\_i2 with other UGT isoforms.*

UGT2A1 $\Delta$ exon3 was cloned into the pcDNA6.2/V5/GW/D-TOPO vector using UGT2A1\_S2 and UGT2A1\_AS2 primers as described above. The newly-created pcDNA6.2/V5/GW/D-TOPO\_UGT2A1 $\Delta$ exon3 vector was transfected using a standard lipofectamine protocol into previously-established stable HEK293 cell lines over-expressing UGT1A7, UGT1A10, or UGT2B17 (Ren et al., 2000; Dellinger et al., 2006; Sun et al., 2006; Chen et al., 2008). The pcDNA6.2/V5/GW/D-TOPO\_wtUGT2A1 vector described above was also transfected into UGT1A10 and UGT2B17 over-expressing cell lines using a standard lipofectamine protocol. Selection of HEK293 cells co-expressing UGT2A1\_i1 or UGT2A1\_i2 and UGT1A7, UGT1A10, or UGT2B17 was completed using blasticidin (9  $\mu$ g/mL) and G418 (400  $\mu$ g/mL).

Following RNA extraction and RT of RNA from the -co-expressing cell lines, real-time PCR was performed to determine the relative levels of UGT1A7, UGT1A10, or UGT2B17 expression versus wild-type UGT2A1 or UGT2A1 $\Delta$ exon3 expression in each

JPET #198770

co-expressed cell line. ABI gene expression assays for UGT1A7 (Hs02517015\_s1), UGT1A10 (Hs02516990\_s1), UGT2B17 (Hs00854486\_sH), and UGT2A1 (Hs00792016\_m1) were used to determine relative transcript levels. The UGT2A1 ABI gene expression assay is specific for UGT2A1 exon 1, enabling the assay to detect transcripts from both the wild-type UGT2A1 and exon 3-deleted UGT2A1 splice variant. Reactions were completed using the standard ABI protocol, with RPLPO used as a housekeeping gene. cDNA corresponding to 20 ng RNA was used for each real-time reaction and reactions were performed in triplicate using standard ABI thermal cycling parameters. Real-time-PCR data was corrected to account for the amplification efficiency of each real-time PCR assay, as described previously (Jones et al., 2012). The relative level of UGT2A1 transcript in each cell line was calculated using the  $\Delta\Delta C_t$  method, relative to the amount of UGT1A7, UGT1A10, or UGT2B17 in each co-expressed cell line. An anti-UGT1A antibody (BD Biosciences; San Jose, CA) at 1:3000 dilution and the V5-HRP antibody described above at 1:5000 dilution were used in Western blot analyses to verify that co-expression had no impact on UGT1A7, UGT1A10, or UGT2A1\_V5 expression.

Homogenate was created from each of the HEK293 co-expressed over-expressing cell lines and glucuronidation assays were completed as described above. Glucuronidation assays were performed using homogenates from HEK293 over-expressing either UGT1A7/UGT2A1\_i2, UGT1A10/UGT2A1\_i2, or UGT2B17/UGT2A1\_i2, with 3-OH-B(a)P and/or 1-naphthol as substrates, as PAHs were previously shown to be glucuronidated by these UGTs (Zheng et al., 2002; Turgeon et al., 2003; Dellinger et al., 2006). Since UGT2A1 exhibits activity against

JPET #198770

PAHs (Bushey et al., 2011), homogenates from HEK293 cells over-expressing UGT1A10/UGT2A1\_i1 and UGT2B17/UGT2A1\_i1 were used in glucuronidation assays with the tobacco specific nitrosamine (TSNA) 4-(methylnitrosamino)-1-(3-pyridyl)-1-butanol (NNAL), which is not a substrate for UGT2A1 but is metabolized by both UGTs 1A10 and 2B17 (Lazarus et al., 2005; Balliet et al., 2010). As previous co-expression studies have reported activity changes to be substrate dependent (Fujiwara et al., 2007; Finel and Kurkela, 2008), additional activity reactions were performed using other non-UGT2A1 substrates, including the flavonoid chrysin for UGT1A7/UGT2A1\_i2 (Webb et al., 2005), the heterocyclic amine (HCA) metabolite *N*-hydroxy-2-amino-1-methyl-6-phenylimidazo[4,5-b]-pyridine (*N*-OH PhIP) for UGT1A10/UGT2A1\_i1 and UGT1A10/UGT2A1\_i2 (Dellinger et al., 2007), and ibuprofen for UGT2B17/UGT2A1\_i1 and UGT2B17/UGT2A1\_i2 (Turgeon et al., 2003). For chrysin, *N*-OH PhIP, and ibuprofen glucuronidation rate determinations, substrate concentrations were chosen which approximated the reported  $K_M$  from previous experiments.

*Data analysis and Statistics.* Three independent experiments were performed for kinetic analyses and GraphPad Prism 5 software was used to calculate kinetic values. Kinetic constants  $V_{max}$  and  $K_M$  for all substrates were calculated using the Michaelis-Menten equation for the rate of product formation versus substrate concentration, with data transformed into linear Eadie-Hofstee plots. An ANOVA, followed by a post test for linear trend, was used to compare the  $K_M$  and  $V_{max}$  of glucuronide formation for the various UGT2A1\_i1 /UGT2A1\_i2 PonA treatment groups. The Students t-test was used

JPET #198770

to compare mRNA expression levels and enzyme kinetics of homogenate activities following co-expression of UGT2A1 with UGT1A7, UGT1A10, or UGT2B17.

## Results

**Relative UGT2A1 $\Delta$ exon3 expression in multiple tissues.** Since its original discovery in olfactory epithelium (Jedlitschky et al., 1999), UGT2A1 has been shown to be expressed in multiple respiratory, digestive, and aerodigestive tract tissues (Bushey et al., 2011). In the present study, RT-PCR amplification of UGT2A1 from pooled lung RNA yielded two distinct products; wild-type UGT2A1 and a novel variant of UGT2A1, which upon direct sequencing was shown to be a splice variant lacking exon 3 (UGT2A1 $\Delta$ exon3; Figure 1, Panel B). The deletion of this exon creates a transcript that is 132 nucleotides shorter, with the open reading frame of the gene remaining intact. Independent PCR amplification and sequencing of genomic DNA from five individual lung specimens containing both the wild-type and variant isoform showed that UGT2A1 had no polymorphisms between exons 2 and 4, inclusive of the exons 2 and 4 splice sites; the lack of prevalent polymorphisms in these regions was confirmed by analyzing this sequence in HapMap (Gibbs, 2003). Following the discovery of this splice variant in lung tissue, additional aerodigestive tract tissues known to express wild-type UGT2A1 were screened for UGT2A1 $\Delta$ exon3 expression. As shown in Figure 1 (Panel C), UGT2A1 $\Delta$ exon3 was also expressed in the trachea, larynx, tonsil, and colon; no UGT2A1 $\Delta$ exon3 expression was observed in pooled olfactory RNA. Using a custom real-time PCR assay (Figure 1, panel A), the relative expression levels of UGT2A1 $\Delta$ exon3 were determined relative to wild-type UGT2A1 in each tissue, with wild-type UGT2A1 expression in each tissue set to 1.0 as a reference. The relative

JPET #198770

UGT2A1 $\Delta$ exon3 expression was demonstrated to be the highest in colon ( $0.79 \pm 0.08$ ), followed by lung ( $0.42 \pm 0.12$ ) > larynx ( $0.39 \pm 0.05$ ) > trachea ( $0.27 \pm 0.07$ ) > tonsil ( $0.10 \pm 0.02$ ) (Figure 1, panel D). In agreement with a previous study analyzing wild-type UGT2A1 expression (Bushey et al., 2011), no UGT2A1 $\Delta$ exon3 expression was detected after multiple RT-PCR attempts or by real-time PCR in tissues of the prostate, liver, pancreas, kidney, esophagus, whole brain, olfactory, or breast (results not shown)

**UGT2A1\_i2 protein expression in a HEK293 over-expressing cell line and in tissue homogenates.** An antibody against UGT2A1 was previously created and used to assess wild-type UGT2A1 (termed 'UGT2A1\_i1') protein levels in HEK293 over-expressing cell lines (Bushey et al., 2011). Similarly, a stable HEK293 cell line transfected with UGT2A1 $\Delta$ exon3 demonstrated UGT2A1 splice variant protein (termed 'UGT2A1\_i2') over-expression using the same antibody (Figure 1, Panel E), with the mean level of UGT2A1\_i1 protein expression calculated to be  $0.92 \pm 0.07$  versus that observed for UGT2A1\_i2 (set as 1.0 as a reference) in the two UGT2A1 over-expressing cell lines. The UGT2A1\_i2 protein lacks 44 amino acids that are derived from exon 3, creating a protein that is 483 amino acids in length compared to the 527 amino acids that comprise UGT2A1\_i1. Expression of both UGT2A1\_i1 and UGT2A1\_i2 were shown in protein homogenates made from normal lung tissues from three donors and normal colon tissues from three donors (Figure 1, Panel F). For the lung and colon specimens analyzed, UGT2A1\_i1 was expressed at marginally higher levels than UGT2A1\_i2, with the ratios of UGT2A1\_i2:UGT2A1\_i1 ranging from 0.6 – 0.9 for lung and 0.5 – 0.7 for colon.

**Enzymatic activity of UGT2A1\_i2.** As UGT2A1 $\Delta$ exon3 RNA and UGT2A1\_i2 protein were shown to be expressed in lung and a variety of other human tissues including tissues of the aerodigestive tract, and because UGT2A1\_i1 was previously shown to be active against PAHs involved in tobacco carcinogenesis (Bushey et al., 2011), UGT2A1\_i2 activity against PAHs and other tobacco carcinogens was investigated. Homogenate from UGT2A1\_i2-over-expressing HEK293 cells, which was shown to express UGT2A1\_i2 protein at slightly higher relative levels than the stable HEK293 cell line over-expressing UGT2A1\_i1 (see Figure 1, Panel E), was used in glucuronidation activity assays to determine the enzymatic activity of UGT2A1\_i2. While cell homogenates over-expressing UGT2A1\_i1 demonstrated glucuronidation activity against both 3-OH-B(a)P (Figure 2, panel A) and 5-methyl-chrysene-1,2-diol (Figure 2, panel C), no glucuronide was detected when UGT2A1\_i2 protein was used in the assay (Figure 2, panels B and D). No detectable glucuronidation activity was observed for UGT2A1\_i2-over-expressing cell homogenates against all other PAHs examined including 1-OH-pyrene, 1-naphthol, 1-OH-B(a)P, 7-OH-B(a)P, 8-OH-B(a)P, B(a)P-7,8-diol, and dibenzo(a,l)pyrene-11,12-diol, using up to 400  $\mu$ g cellular homogenate and 750  $\mu$ M substrate in a 18 h incubation (results not shown). The UGT2A1\_i2 variant also lacked activity against 4-MU, a known UGT2A1 substrate and a common substrate of most UGT isoforms (Uchaipichat et al., 2004). UGT2A1\_i1 was previously shown to have no detectable glucuronidation activity against TSNA and HCAs (Bushey et al., 2011); UGT2A1\_i2 also had no detectable glucuronidation activity against these substrates (results not shown).

**UGT2A1\_i2 modulates UGT2A1\_i1 activity.** To examine the potential effects of increasing levels of UGT2A1\_i2 expression on UGT2A1\_i1 activity, a co-expression system was generated to allow for stable UGT2A1\_1 protein levels and UGT2A1\_2 expression levels regulated by the ecdysone analog PonA. In order to more easily differentiate between the UGT2A1 isomers in co-IP experiments, UGT2A1\_i1 was V5-tagged and UGT2A1\_i2 was FLAG-tagged, both at the C-terminus of the protein. As shown by Western blot analysis (Figure 3, Panel A), no detectable expression of UGT2A1\_i2\_FLAG was observed in the vehicle control group. Following the addition of increasing dosages of PonA there was a corresponding increase in UGT2A1\_i2\_FLAG levels while UGT2A1\_i1\_V5 levels remained relatively constant. The UGT2A1\_i2 induction and corresponding protein quantification was completed in triplicate: 2  $\mu$ M PonA treatment induced the mean UGT2A1\_i2 levels to  $0.28 \pm 0.05$  relative to UGT2A1\_i1 (set as 1.0 as a reference in all cases), 6  $\mu$ M PonA treatment induced the mean UGT2A1\_i2 levels to  $0.76 \pm 0.06$  relative to UGT2A1\_i1, and 10  $\mu$ M PonA treatment induced the mean UGT2A1\_i2 levels to  $1.18 \pm 0.09$  relative to UGT2A1\_i1. Relative UGT2A1\_i1\_V5 protein levels were calculated for each treatment group and used for normalization of kinetic data, with UGT2A1\_i1 expression in the control group set as the reference at 1.0. UGT2A1\_i1 expression was relatively consistent in all treatment groups (Figure 3, Panel A). Mean UGT2A1\_i1\_V5 levels were determined to be  $0.89 \pm 0.08$  in the 2  $\mu$ M PonA treatment group,  $0.95 \pm 0.06$  in the 6  $\mu$ M PonA treatment group, and  $0.94 \pm 0.04$  in the 10  $\mu$ M PonA treatment group. UGT2A1\_i1\_V5 and UGT2A1\_i2\_FLAG expression levels were confirmed by Western blot using the



JPET #198770

anti-UGT2A1 antibody (Figure 3, Panel B). Using this antibody, no UGT2A1\_i2 was detected in the control group and the ratio of UGT2A1\_i2:UGT2A1\_i1 in the 10  $\mu$ M treatment group (1.1) was approximately equal to that observed using the anti-FLAG and anti-V5 antibodies ( $1.18 \pm 0.09$ ) described above. In addition, the relative expression of UGT2A1\_i1 in the 10  $\mu$ M PonA treatment group using the anti-UGT2A1 antibody (0.97) was similar to that observed using the anti-FLAG and anti-V5 antibodies ( $0.94 \pm 0.04$ ) described above.

Activity assays and enzyme kinetics were completed to determine the potential impact of UGT2A1\_i2 expression on UGT2A1\_i1 enzyme activity. The effects of UGT2A1\_i2 expression on UGT2A1\_i1 activity were assessed in glucuronidation assays using the PAH substrates 1-OH-pyrene, 3-OH-B(a)P, and B(a)P-7,8-diol. These substrates represent PAHs of varying complexity and were all shown to be substrates for UGT2A1\_i1 in previous studies (Bushey et al., 2011). Representative chromatograms using cell homogenates from the control group and the three PonA treatment groups against 1-OH-pyrene (Figure 3, Panel C) and Michaelis-Menten kinetics curves for three PAHs examined (Figure 3, Panel D) show that increases in UGT2A1\_i2 expression caused a decrease in the rate of UGT2A1\_i1 glucuronide formation. Upon kinetic analysis, significant ( $p < 0.01$ ) trends were observed between increasing levels of UGT2A1\_i2 expression and decreasing PAH-glucuronide formation as determined by  $V_{max}$  and  $V_{max}/K_M$  for each of the three substrates analyzed (Table 1). Homogenate from cells with the highest UGT2A1\_i2 expression, which exhibited a UGT2A1\_i2:UGT2A1\_i1 ratio of approximately 1.2, had a ~50% reduction in glucuronide formation for all three substrates examined. No significant changes in  $K_M$

JPET #198770

values were observed when UGT2A1\_i2 expression was induced, regardless of UGT2A1\_i2 expression levels. PonA treatment had no effect on the glucuronidation activity of homogenates expressing UGT2A1\_i1 against 1-OH-pyrene (results not shown). The C-terminal V5 tag caused no significant changes in UGT2A1 enzyme activity (data not shown), with the enzyme kinetics ( $V_{max}$  and  $K_M$ ) for the control UGT2A1\_i1\_V5-over-expressing cell homogenates in these experiments similar to those reported previously for untagged UGT2A1 against PAHs (Bushey et al., 2011).

**UGT2A1\_i1 and UGT2A1\_i2 hetero-oligomerization.** To test whether UGT2A1\_i2 potentially modulates UGT2A1\_i1 glucuronidation activity by a direct protein-protein interaction, protein lysate from cells treated with 10  $\mu$ M PonA was used in co-IP experiments. Using an anti-FLAG antibody to immunoprecipitate UGT2A1\_i2\_FLAG and an anti-V5 antibody to detect UGT2A1\_i1\_V5 by Western blot analysis, a band corresponding to UGT2A1\_i1\_V5 (~57 kDa) was observed (Figure 4, Panel A; lane 5). As expected, a UGT2A1\_i1\_V5 band was observed using the anti-V5 antibody by Western blot analysis when an anti-V5 antibody was used to pull down UGT2A1\_i1\_V5 (Figure 4, Panel A; lane 4); no bands were observed when no antibody was added to the immunoprecipitation lysate (Figure 4, Panel A; lane 3) or when lysate was used from HEK293 cell lines over-expressing either UGT2A1\_i1\_V5 or UGT2A1\_i2\_FLAG alone (Figure 4, Panel A; lanes 1-2). Similarly, a band corresponding to UGT2A1\_i2\_FLAG (~52 kDa) was detected when an anti-V5 antibody was used to immunoprecipitate UGT2A1\_i1\_V5 and an anti-Flag antibody was used to detect UGT2A1\_i2\_FLAG by Western blot (Figure 4, Panel B; lane 5). Again as

JPET #198770

expected, an UGT2A1\_i2\_FLAG band was observed by Western blot analysis when an anti-FLAG antibody was used to pull down UGT2A1\_i2\_FLAG (Figure 4, Panel B; lane 4); no bands were observed when no antibody was added to the immunoprecipitation lysate (Figure 4, Panel B; lane 3) or when lysate was used from HEK293 cell lines over-expressing either UGT2A1\_i1\_V5 or UGT2A1\_i2\_FLAG alone (Figure 4, Panel B; lanes 1-2).

**UGT2A1\_i1 homo-oligomerization.** As UGT2A1\_i1 and UGT2A1\_i2 were shown to form hetero-oligomers, experiments were conducted to determine whether UGT2A1\_i1 homo-oligomerization also occurs. As described in the Materials and Methods, a stable HEK293 cell line was created to co-express UGT2A1\_i1\_V5 and UGT2A1\_i1\_FLAG. Following treatment with 10  $\mu$ M PonA, the levels of UGT2A1\_i1\_FLAG were induced to approximately the same levels as UGT2A1\_i1\_V5, while no UGT2A1\_i1\_FLAG expression was observed in the vehicle control group (Figure 5, Panel A). UGT2A1\_i1\_V5 and UGT2A1\_i1\_FLAG expression levels were confirmed to be relatively equal following Western blot analysis using the anti-UGT2A1 antibody (Figure 5, Panel B). Using an anti-FLAG antibody to immunoprecipitate UGT2A1\_i1\_FLAG and an anti-V5-HRP antibody to detect UGT2A1\_i1\_V5 by Western blot analysis, a band corresponding to UGT2A1\_i1\_V5 was detected (Figure 5, Panel C; lane 5). Background bands at an approximate size of 45 kDa were observed in lanes 4 and 5 in all cases when homo-oligomerization was investigated using an anti-FLAG antibody to immunoprecipitate the complex and an anti-V5-HRP antibody for Western blot; the cause of these background signals is unknown. Similarly, a band

JPET #198770

corresponding to UGT2A1\_i1\_FLAG was detected when an anti-V5 antibody was used to immunoprecipitate UGT2A1\_i1\_V5 and an anti-Flag-HRP antibody was used to detect UGT2A1\_i1\_FLAG by Western blot (Figure 5, Panel D; lane 5). Positive and negative controls, identical to those described in detail for UGT2A1\_i1 and UGT2A1\_i2 hetero-oligomerization, were used.

**Effect of UGT2A1\_i1 or UGT2A1\_i2 co-expression on the glucuronidation activities other UGT isoforms.** To examine whether UGT2A1 isoforms potentially modulate the activity of other UGTs, studies were performed co-expressing either UGT2A1\_i1\_V5 or UGT2A1\_i2\_V5 with UGTs 1A7, 1A10, or 2B17. These UGTs were chosen because they are expressed in the respiratory and/or aerodigestive tract and are active against tobacco carcinogens (Zheng et al., 2002; Dellinger et al., 2006; Gallagher et al., 2007). As determined by real-time PCR, the relative levels of transcript in each UGT-co-expressing cell line were not significantly different for the UGT2A1 isoform as compared to its UGT1A or 2B counterpart (Figure 6, Panel A). Western blots demonstrated that UGTs 1A7 and 1A10 were expressed at similar levels when over-expressed alone or when co-expressed with UGT2A1, and that similar levels of UGT2A1\_i1\_V5 and UGT2A1\_i2\_V5 protein were observed in each co-expressed over-expressing cell line (data not shown).

Glucuronidation assays were performed using protein from cells over-expressing UGT1A or UGT2B enzymes alone or after co-expression with UGT2A1 isoforms. Representative Michaelis-Menten curves for UGT1A7- and UGT1A7/UGT2A1\_i2 -over-expressing cell homogenates show similar kinetics against 3-OH-BaP (Figure 6, Panel

JPET #198770

B). A similar pattern was observed for UGT1A10- and UGT1A10/UGT2A1\_i2 -over-expressing cell homogenates against 3-OH-BaP and for UGT2B17- and UGT2B17/UGT2A1\_i2 -over-expressing cell homogenates against 1-naphthol (Figure 6, Panel B). Glucuronidation assays also showed no significant changes in glucuronidation activity for UGT1A10- and UGT1A10/UGT2A1\_i1 -over-expressing cell homogenates and UGT2B17- and UGT2B17/UGT2A1\_i1 -over-expressing cell homogenates against the non-UGT2A1 substrate NNAL (results not shown). No significant differences in  $K_M$  or  $V_{max}$  were observed for any substrate analyzed after UGT1A or 2B co-expression with either UGT2A1\_i2 or UGT2A1\_i1. No significant differences in glucuronidation rates of additional substrates were observed using homogenates from cells co-expressing UGTs 1A7, 1A10, or 2B17 and UGT2A1; this included glucuronidation of the flavonoid chrysin by the UGT1A7 co-expressing cell line, glucuronidation of the HCA metabolite *N*-OH PhIP by the UGT1A10 co-expressing cell lines, and glucuronidation of ibuprofen by the UGT2B17 co-expressing cell lines (data not shown). In addition, UGT2A1\_i1 activity against testosterone and the PAH, 5-methylchrysene-1,2-diol, was unchanged following co-expression with UGT1A10 or UGT2B17, respectively (data not shown).

## Discussion

The present study is the first to identify and characterize a novel splice variant of UGT2A1, demonstrating its expression in multiple tissues at both the level of mRNA and protein and its functional importance as an inhibitor of UGT2A1 activity. This variant consists of a deletion of exon 3 that results in an inactive UGT2A1 isoform. UGT2A1 exon 3 is a conserved region throughout all UGT family members (Nagar and Rimmel, 2006) and is also highly conserved with the corresponding region of the mouse ortholog UGT2a1 following sequence alignment. The exon 3-encoded protein region of all UGTs is hypothesized to form a portion of the UDPGA co-substrate binding pocket necessary for UGT function, and similar to the activity results for the splice variant UGT2A1 isoform in the present study, amino acid point mutations in this region have been previously shown to ablate UGT enzyme activity (Miley et al., 2007; Laakkonen and Finel; Bushey et al., 2011).

In addition to possessing no detectable glucuronidation activity, UGT2A1\_i2 was shown to act as a negative regulator of UGT2A1\_i1 activity. This negative regulatory effect is similar to that observed for other UGT splice variants, including inactive UGT1A splice variants with an alternate exon 5b at the 3' end of the UGT1A transcript (Girard et al., 2007; Levesque et al., 2007). This negative inhibition appears to be due to direct binding of the inactive UGT2A1\_i2 variant with UGT2A1\_i1, a mechanism similar to that observed for other UGTs including the UGT1A exon 5b variant (Bellemare et al., 2010). Further, a Gln331Stop polymorphism in UGT1A1 leads to a truncated and inactive protein, and this protein isoform has been reported to bind to and inhibit wild-type

JPET #198770

UGT1A1 activity (Koiwai et al., 1996). Ghosh et al. showed that an inactive mutant form of UGT1A1, caused by a single amino acid change at codon 127, could bind to and inhibit wild-type UGT1A1 activity in a dominant-negative manner (Ghosh et al., 2001). Also, recent work has identified inactive UGT2B4 splice variant isoforms that negatively regulate wild-type UGT2B4 activity (Levesque et al., 2010), and inactive UGT2B7 splice variant isoforms negatively modulate wild-type UGT2B7 activity (Menard et al., 2011).

In the present study, a PonA-inducible co-expression system was designed to control UGT2A1\_i2 expression so that its effects on UGT2A1\_i1 activity could be examined. A linear correlation was observed between the ratio of UGT2A1\_i2:UGT2A1\_i1 expression and overall glucuronidation activity of homogenates from co-expressed cells. At the highest level of UGT2A1\_i2 induction, with the expression of UGT2A1\_i2 approximately equal to that of UGT2A1\_i1, there was an approximately 50% reduction in the rate of glucuronide formation for three PAH substrates examined. As the UGT2A1\_i2:UGT2A1\_i1 ratio decreased, proportional increases in UGT2A1\_i1 activity were observed against all three PAH substrates. These data suggest that UGT2A1\_i1 interacts with UGT2A1\_i2 in a 1:1 stoichiometry, likely as a dimer as proposed for other UGTs (Finel and Kurkela, 2008; Bellemare et al., 2010). The *in vitro* inducible UGT2A1\_i2:UGT2A1\_i1 ratios observed in this study approximated the ratios observed physiologically in several human tissues including lung and colon. These UGT2A1\_i2:UGT2A1\_i1 ratios corresponded with 10-50% decreases in the  $V_{max}$  for UGT2A1\_i1-mediated glucuronidation activities against PAH substrates; no significant change in UGT2A1\_i1  $K_M$  due to UGT2A1\_i2 co-expression was observed. These data suggest that the inhibitory effect of UGT2A1\_i2 expression is

JPET #198770

mediated by removal of UGT2A1\_i1 from the active protein pool, rather than an effect on UGT2A1\_i1 enzyme-substrate affinity.

UGTs have been shown to reside in the endoplasmic reticulum to form both homo- and hetero-oligomers (Fujiwara et al., 2007; Operana and Tukey, 2007; Finel and Kurkela, 2008). *In vitro* UGT co-expression and oligomerization studies have shown that UGT interactions are complex, with kinetic changes dependent on the specific UGT isoforms interacting and the substrates undergoing glucuronidation (Fujiwara et al., 2007; Operana and Tukey, 2007; Finel and Kurkela, 2008). The co-IP experiments presented in this study suggested hetero-oligomerization occurs between the UGT2A1\_i1 and UGT2A1\_i2 isoforms, and UGT2A1 homo-oligomerization was also investigated. *In vitro* co-IP experiments showed for the first time that UGT2A1\_i1 homo-oligomerization does in fact occur. UGT2A1 co-expression studies were completed with two members of the UGT1A sub-family, UGT1A7 and UGT1A10, and UGT2B17 to determine any UGT2A1-mediated changes in UGT1A or UGT2B glucuronidation activity. Like UGT2A1, UGTs 1A7, 1A10, and 2B17 are expressed in certain tissues of the respiratory and aerodigestive tract and exhibit glucuronidation activity against multiple tobacco carcinogens (Zheng et al., 2002; Dellinger et al., 2006; Dellinger et al., 2007; Gallagher et al., 2007). UGT2A1 was determined to have no effect on the glucuronidation activity of UGT1A7, UGT1A10 or UGT2B17 against tobacco carcinogens, including PAHs, TSNAs and HCAs, suggesting that UGT2A1 does not affect the ability of these UGTs to detoxify tobacco carcinogens *in vivo* and that UGT2A1\_i2 regulation of UGT activity is UGT2A1-specific.



JPET #198770

The entire UGT2A family has been understudied, with limited information reported on expression and activity of these enzymes. UGT2A3 has been shown to be well expressed in the colon, small intestine and liver, with activity reported against bile acids (Court et al., 2008). UGT2A2 has been reported to be expressed in the nasal mucosa, with broad substrate selectivity reported against various estrogen and phenylphenol metabolites (Sneitz et al., 2009). Neither of these enzymes has been carefully investigated for aerodigestive tract expression or metabolism against carcinogens, and this will be investigated in future studies. UGT2A1 and UGT2A2 have both been shown to exhibit glucuronidation activity against similar substrates, with UGT2A1 generally having higher glucuronidation rates (Sneitz et al., 2009). Based on exon sharing of exon 1 of UGT2A1 or UGT2A2 to common exons 2-6, the same exon 3 deletion splice variant for UGT2A2 is likely to occur. Future studies are planned to determine whether the UGT2A2 $\Delta$ exon3 variant exists and, if so, the expression and functional implications of this UGT2A2 variant will be examined.

The novel UGT2A1<sub>i2</sub> regulatory mechanism described here may allow for tighter control of UGT2A1 glucuronidation activity. The expression of both UGT2A1<sub>i1</sub> and UGT2A1<sub>i2</sub> in multiple human tissues suggests widespread physiological importance, particularly as it relates to tobacco-related cancer susceptibility. We hypothesize that the balance between active UGT2A1<sub>i1</sub> and inactive UGT2A1<sub>i2</sub> could influence carcinogen metabolism in local tissues susceptible to tobacco-induced carcinogenesis, with individuals expressing higher amounts of UGT2A1<sub>i2</sub> potentially exhibiting higher susceptibility to tobacco related cancers of the respiratory and aerodigestive tracts. The potential influence of a UGT2A1 splicing variant on cancer risk

JPET #198770

could also complicate the findings of genetic epidemiologic studies (including genome-wide association studies) of UGT2A1, which exhibits at least two prevalent (>4%) polymorphisms that alter UGT2A1 enzymatic activity (Bushey et al., 2011). Further studies examining the involvement of UGT2A1 genetic and splicing variants on cancer susceptibility are currently underway.

JPET #198770

## **Acknowledgements**

We thank the Functional Genomics Core Facility at the Penn State University College of Medicine for real-time PCR services, the Nucleic Acid Facility at Penn State University for DNA sequencing services, and the Organic Synthesis Core Facility at Penn State University College of Medicine for providing tobacco carcinogens for this study.

JPET #198770

### **Authorship Contributions**

*Participated in research design:* Bushey, Lazarus

*Conducted experiments:* Bushey

*Contributed new reagents of analytic tools:* Bushey, Lazarus

*Performed data analysis:* Bushey, Lazarus

*Wrote or contributed to writing of the manuscript:* Bushey, Lazarus

## References

- Balliet RM, Chen G, Dellinger RW and Lazarus P (2010) UDP-glucuronosyltransferase 1A10: activity against the tobacco-specific nitrosamine, 4-(methylnitrosamino)-1-(3-pyridyl)-1-butanol, and a potential role for a novel UGT1A10 promoter deletion polymorphism in cancer susceptibility. *Drug Metab Dispos* **38**:484-490.
- Balliet RM, Chen G, Gallagher CJ, Dellinger RW, Sun D and Lazarus P (2009) Characterization of UGTs active against SAHA and association between SAHA glucuronidation activity phenotype with UGT genotype. *Cancer Res* **69**:2981-2989.
- Bellemare J, Rouleau M, Harvey M and Guillemette C (2010) Modulation of the human glucuronosyltransferase UGT1A pathway by splice isoform polypeptides is mediated through protein-protein interactions. *J Biol Chem* **285**:3600-3607.
- Bushey RT, Chen G, Blevins-Primeau AS, Krzeminski J, Amin S and Lazarus P (2011) Characterization of UDP-glucuronosyltransferase 2A1 (UGT2A1) variants and their potential role in tobacco carcinogenesis. *Pharmacogenet Genomics* **21**:55-65.
- Chen G, Dellinger RW, Gallagher CJ, Sun D and Lazarus P (2008) Identification of a prevalent functional missense polymorphism in the UGT2B10 gene and its association with UGT2B10 inactivation against tobacco-specific nitrosamines. *Pharmacogenet Genomics* **18**:181-191.

JPET #198770

- Court MH, Hazarika S, Krishnaswamy S, Finel M and Williams JA (2008) Novel polymorphic human UDP-glucuronosyltransferase 2A3: cloning, functional characterization of enzyme variants, comparative tissue expression, and gene induction. *Mol Pharmacol* **74**:744-754.
- Dellinger RW, Chen G, Blevins-Primeau AS, Krzeminski J, Amin S and Lazarus P (2007) Glucuronidation of PhIP and N-OH-PhIP by UDP-glucuronosyltransferase 1A10. *Carcinogenesis* **28**:2412-2418.
- Dellinger RW, Fang JL, Chen G, Weinberg R and Lazarus P (2006) Importance of UDP-glucuronosyltransferase 1A10 (UGT1A10) in the detoxification of polycyclic aromatic hydrocarbons: decreased glucuronidative activity of the UGT1A10139Lys isoform. *Drug Metab Dispos* **34**:943-949.
- Fang JL, Beland FA, Doerge DR, Wiener D, Guillemette C, Marques MM and Lazarus P (2002) Characterization of benzo(a)pyrene-trans-7,8-dihydrodiol glucuronidation by human tissue microsomes and overexpressed UDP-glucuronosyltransferase enzymes. *Cancer Res* **62**:1978-1986.
- Finel M and Kurkela M (2008) The UDP-glucuronosyltransferases as oligomeric enzymes. *Curr Drug Metab* **9**:70-76.
- Fujiwara R, Nakajima M, Yamanaka H, Katoh M and Yokoi T (2007) Interactions between human UGT1A1, UGT1A4, and UGT1A6 affect their enzymatic activities. *Drug Metab Dispos* **35**:1781-1787.

JPET #198770

Gallagher CJ, Muscat JE, Hicks AN, Zheng Y, Dyer AM, Chase GA, Richie J and

Lazarus P (2007) The UDP-glucuronosyltransferase 2B17 gene deletion polymorphism: sex-specific association with urinary 4-(methylnitrosamino)-1-(3-pyridyl)-1-butanol glucuronidation phenotype and risk for lung cancer. *Cancer Epidemiol Biomarkers Prev* **16**:823-828.

Ghosh SS, Sappal BS, Kalpana GV, Lee SW, Chowdhury JR and Chowdhury NR

(2001) Homodimerization of human bilirubin-uridine-diphosphoglucuronate glucuronosyltransferase-1 (UGT1A1) and its functional implications. *J Biol Chem* **276**:42108-42115.

Gibbs RA (2003) The International HapMap Project. *Nature* **426**:789-796.

Girard H, Levesque E, Bellemare J, Journault K, Caillier B and Guillemette C (2007)

Genetic diversity at the UGT1 locus is amplified by a novel 3' alternative splicing mechanism leading to nine additional UGT1A proteins that act as regulators of glucuronidation activity. *Pharmacogenet Genomics* **17**:1077-1089.

Itaaho K, Mackenzie PI, Ikushiro S, Miners JO and Finel M (2008) The configuration of

the 17-hydroxy group variably influences the glucuronidation of beta-estradiol and epiestradiol by human UDP-glucuronosyltransferases. *Drug Metab Dispos* **36**:2307-2315.

Jedlitschky G, Cassidy AJ, Sales M, Pratt N and Burchell B (1999) Cloning and

characterization of a novel human olfactory UDP-glucuronosyltransferase. *Biochem J* **340 ( Pt 3)**:837-843.

JPET #198770

- Jin CJ, Miners JO, Burchell B and Mackenzie PI (1993) The glucuronidation of hydroxylated metabolites of benzo[a]pyrene and 2-acetylaminofluorene by cDNA-expressed human UDP-glucuronosyltransferases. *Carcinogenesis* **14**:2637-2639.
- Jones NR, Sun D, Freeman WM and Lazarus P (2012) Quantification of hepatic UGT1A splice variant expression and correlation of UGT1A1 variant expression with glucuronidation activity. *J Pharmacol Exp Ther*.
- Koiwai O, Aono S, Adachi Y, Kamisako T, Yasui Y, Nishizawa M and Sato H (1996) Crigler-Najjar syndrome type II is inherited both as a dominant and as a recessive trait. *Hum Mol Genet* **5**:645-647.
- Laakkonen L and Finel M (2010) A molecular model of the human UDP-glucuronosyltransferase 1A1, its membrane orientation, and the interactions between different parts of the enzyme. *Mol Pharmacol* **77**:931-939.
- Lander ES, Linton LM, Birren B, Nusbaum C, Zody MC, Baldwin J, Devon K, Dewar K, Doyle M, FitzHugh W, Funke R, Gage D, Harris K, Heaford A, Howland J, Kann L, Lehoczky J, LeVine R, McEwan P, McKernan K, Meldrim J, Mesirov JP, Miranda C, Morris W, Naylor J, Raymond C, Rosetti M, Santos R, Sheridan A, Sougnez C, Stange-Thomann N, Stojanovic N, Subramanian A, Wyman D, Rogers J, Sulston J, Ainscough R, Beck S, Bentley D, Burton J, Clee C, Carter N, Coulson A, Deadman R, Deloukas P, Dunham A, Dunham I, Durbin R, French L, Grafham D, Gregory S, Hubbard T, Humphray S, Hunt A, Jones M, Lloyd C, McMurray A, Matthews L, Mercer S, Milne S, Mullikin JC, Mungall A, Plumb R, Ross M, Shownkeen R, Sims S, Waterston RH, Wilson RK, Hillier LW, McPherson JD, Marra MA, Mardis ER, Fulton LA, Chinwalla AT, Pepin KH, Gish



JPET #198770

- WR, Chissoe SL, Wendl MC, Delehaunty KD, Miner TL, Delehaunty A, Kramer JB, Cook LL, Fulton RS, Johnson DL, Minx PJ, Clifton SW, Hawkins T, Branscomb E, Predki P, Richardson P, Wenning S, Slezak T, Doggett N, Cheng JF, Olsen A, Lucas S, Elkin C, Uberbacher E, Frazier M, et al. (2001) Initial sequencing and analysis of the human genome. *Nature* **409**:860-921.
- Lazarus P, Zheng Y, Aaron Runkle E, Muscat JE and Wiener D (2005) Genotype-phenotype correlation between the polymorphic UGT2B17 gene deletion and NNAL glucuronidation activities in human liver microsomes. *Pharmacogenet Genomics* **15**:769-778.
- Levesque E, Girard H, Journault K, Lepine J and Guillemette C (2007) Regulation of the UGT1A1 bilirubin-conjugating pathway: role of a new splicing event at the UGT1A locus. *Hepatology* **45**:128-138.
- Levesque E, Menard V, Laverdiere I, Bellemare J, Barbier O, Girard H and Guillemette C (2010) Extensive splicing of transcripts encoding the bile acid-conjugating enzyme UGT2B4 modulates glucuronidation. *Pharmacogenet Genomics* **20**:195-210.
- Mackenzie PI, Bock KW, Burchell B, Guillemette C, Ikushiro S, Iyanagi T, Miners JO, Owens IS and Nebert DW (2005) Nomenclature update for the mammalian UDP glycosyltransferase (UGT) gene superfamily. *Pharmacogenet Genomics* **15**:677-685.

JPET #198770

Menard V, Eap O, Roberge J, Harvey M, Levesque E and Guillemette C (2011)

Transcriptional diversity at the UGT2B7 locus is dictated by extensive pre-mRNA splicing mechanisms that give rise to multiple mRNA splice variants.

*Pharmacogenet Genomics* **21**:631-641.

Miley MJ, Zielinska AK, Keenan JE, Bratton SM, Radomska-Pandya A and Redinbo

MR (2007) Crystal structure of the cofactor-binding domain of the human phase II drug-metabolism enzyme UDP-glucuronosyltransferase 2B7. *J Mol Biol* **369**:498-511.

Nagar S and Remmel RP (2006) Uridine diphosphoglucuronosyltransferase

pharmacogenetics and cancer. *Oncogene* **25**:1659-1672.

Nishimura M and Naito S (2006) Tissue-specific mRNA expression profiles of human

phase I metabolizing enzymes except for cytochrome P450 and phase II metabolizing enzymes. *Drug Metab Pharmacokinet* **21**:357-374.

Olson KC, Dellinger RW, Zhong Q, Sun D, Amin S, Spratt TE and Lazarus P (2009)

Functional characterization of low-prevalence missense polymorphisms in the UDP-glucuronosyltransferase 1A9 gene. *Drug Metab Dispos* **37**:1999-2007.

Operana TN and Tukey RH (2007) Oligomerization of the UDP-glucuronosyltransferase

1A proteins: homo- and heterodimerization analysis by fluorescence resonance energy transfer and co-immunoprecipitation. *J Biol Chem* **282**:4821-4829.

Ren Q, Murphy SE, Zheng Z and Lazarus P (2000) O-Glucuronidation of the lung

carcinogen 4-(methylnitrosamino)-1-(3-pyridyl)-1-butanol (NNAL) by human UDP-glucuronosyltransferases 2B7 and 1A9. *Drug Metab Dispos* **28**:1352-1360.

JPET #198770

- Ritter JK, Chen F, Sheen YY, Tran HM, Kimura S, Yeatman MT and Owens IS (1992) A novel complex locus UGT1 encodes human bilirubin, phenol, and other UDP-glucuronosyltransferase isozymes with identical carboxyl termini. *J Biol Chem* **267**:3257-3261.
- Sneitz N, Court MH, Zhang X, Laajanen K, Yee KK, Dalton P, Ding X and Finel M (2009) Human UDP-glucuronosyltransferase UGT2A2: cDNA construction, expression, and functional characterization in comparison with UGT2A1 and UGT2A3. *Pharmacogenet Genomics*.
- Sten T, Bichlmaier I, Kuuranne T, Leinonen A, Yli-Kauhaluoma J and Finel M (2009) UDP-glucuronosyltransferases (UGTs) 2B7 and UGT2B17 display converse specificity in testosterone and epitestosterone glucuronidation, whereas UGT2A1 conjugates both androgens similarly. *Drug Metab Dispos* **37**:417-423.
- Sun D, Chen G, Dellinger RW, Duncan K, Fang JL and Lazarus P (2006) Characterization of tamoxifen and 4-hydroxytamoxifen glucuronidation by human UGT1A4 variants. *Breast Cancer Res* **8**:R50.
- Sun D, Sharma AK, Dellinger RW, Blevins-Primeau AS, Balliet RM, Chen G, Boyiri T, Amin S and Lazarus P (2007) Glucuronidation of active tamoxifen metabolites by the human UDP glucuronosyltransferases. *Drug Metab Dispos* **35**:2006-2014.
- Turgeon D, Carrier JS, Chouinard S and Belanger A (2003) Glucuronidation activity of the UGT2B17 enzyme toward xenobiotics. *Drug Metab Dispos* **31**:670-676.

JPET #198770

- Uchaipichat V, Mackenzie PI, Guo XH, Gardner-Stephen D, Galetin A, Houston JB and Miners JO (2004) Human udp-glucuronosyltransferases: isoform selectivity and kinetics of 4-methylumbelliferone and 1-naphthol glucuronidation, effects of organic solvents, and inhibition by diclofenac and probenecid. *Drug Metab Dispos* **32**:413-423.
- Wang ET, Sandberg R, Luo S, Khrebtukova I, Zhang L, Mayr C, Kingsmore SF, Schroth GP and Burge CB (2008) Alternative isoform regulation in human tissue transcriptomes. *Nature* **456**:470-476.
- Webb LJ, Miles KK, Auyeung DJ, Kessler FK and Ritter JK (2005) Analysis of substrate specificities and tissue expression of rat UDP-glucuronosyltransferases UGT1A7 and UGT1A8. *Drug Metab Dispos* **33**:77-82.
- Wells PG, Mackenzie PI, Chowdhury JR, Guillemette C, Gregory PA, Ishii Y, Hansen AJ, Kessler FK, Kim PM, Chowdhury NR and Ritter JK (2004) Glucuronidation and the UDP-glucuronosyltransferases in health and disease. *Drug Metab Dispos* **32**:281-290.
- Wiener D, Doerge DR, Fang JL, Upadhyaya P and Lazarus P (2004a) Characterization of N-glucuronidation of the lung carcinogen 4-(methylnitrosamino)-1-(3-pyridyl)-1-butanol (NNAL) in human liver: importance of UDP-glucuronosyltransferase 1A4. *Drug Metab Dispos* **32**:72-79.
- Wiener D, Fang JL, Dossett N and Lazarus P (2004b) Correlation between UDP-glucuronosyltransferase genotypes and 4-(methylnitrosamino)-1-(3-pyridyl)-1-butanone glucuronidation phenotype in human liver microsomes. *Cancer Res* **64**:1190-1196.

JPET #198770

Zheng Z, Fang JL and Lazarus P (2002) Glucuronidation: an important mechanism for detoxification of benzo[a]pyrene metabolites in aerodigestive tract tissues. *Drug Metab Dispos* **30**:397-403.

JPET #198770

## Footnotes

---

**Funding:** This work was supported by the National Institutes of Health, National Institute of Dental and Craniofacial Research [Grant R01-DE13158 to P. Lazarus]; and the Pennsylvania Department of Health's Health Research Formula Funding Program [Grants 4100038714 to P. Lazarus, and 4100038715 to S. Whitehead].

**Reprint requests:** Philip Lazarus, Ph.D., Mail Code CH-69, 500 University Drive, Hershey, PA, 17033; plazarus@psu.edu

## Figure Legends

**Figure 1. Determination of UGT2A1 $\Delta$ exon3 expression. (A)** Schematic of quantitative real-time PCR assay developed to specifically detect either wild-type UGT2A1 or UGT2A1 $\Delta$ exon3. **(B)** Full-length UGT2A1 was PCR-amplified following RT of pooled lung RNA. A UGT2A1 mRNA variant lacking exon 3 (UGT2A1 $\Delta$ exon3), in addition to wild-type UGT2A1 mRNA, was discovered following gel extraction and dideoxy sequencing of the PCR products. **(C)** A sense primer specific to exon 1 and an antisense primer specific to exon 5 of UGT2A1 were used in RT-PCR to determine tissue-specific expression of UGT2A1 $\Delta$ exon3 in tissues that were previously determined to express wild-type UGT2A1 (Bushey et al., 2011). For both RT-PCR experiments (panels B and C), the cDNA equivalent of 100 ng RNA was used. RNAs from HEK293 cell lines over-expressing wild-type UGT2A1 or UGT2A1 $\Delta$ exon3 were used as a positive control, while water in place of cDNA was used as a negative control. **(D)** Quantitative real-time PCR was completed to determine UGT2A1 $\Delta$ exon3 expression levels relative to wild-type UGT2A1 expression in human tissues. cDNAs, corresponding to 20 ng of RNAs from tissues exhibiting UGT2A1 $\Delta$ exon3 expression (panels B and C), were used in conjunction with the custom-designed real-time PCR assay described in panel A. Relative UGT2A1 $\Delta$ exon3 expression in each tissue was determined by comparing UGT2A1 $\Delta$ exon3 mRNA levels to wild-type UGT2A1 mRNA levels, set to 1.0 as a reference. Results, expressed as the mean  $\pm$  SD of triplicates, were normalized to RPLPO RNA expression for each tissue. **(E)** Representative Western blot showing UGT2A1<sub>i2</sub> expression in an over-expressing HEK293 cell line.

JPET #198770

50  $\mu\text{g}$  of total protein homogenate from cell lines over-expressing UGT2A1\_i1 or UGT2A1\_i2 was loaded to each lane for a Western blot, and expression was determined using an anti-UGT2A1 antibody.  $\beta$ -actin was used as a loading control. The relative ratio of UGT2A1\_i1 or UGT2A1\_i2 protein to  $\beta$ -actin was used to determine relative protein expression in each over-expressing cell line. **(F)** Lung and colon tissue homogenates (250  $\mu\text{g}$ ) were screened for UGT2A1\_i1 and UGT2A1\_i2 expression; 60  $\mu\text{g}$  of protein (30  $\mu\text{g}$  of each UGT2A1 isoform) from HEK293 cell lines over-expressing UGT2A1\_i1 or UGT2A1\_i2 was mixed in a 1:1 ratio and used as a positive control.  $\beta$ -actin was used as a loading control.

**Figure 2. UGT2A1\_i2 exhibits no detectable glucuronidation activity against various PAHs.** UGT2A1\_i2 activity was determined against PAHs that were previously determined to be substrates of UGT2A1\_i1. Shown are representative UPLC chromatograms of **(A)** UGT2A1\_i1 activity against 3-OH-B(a)P, **(B)** UGT2A1\_i2 activity against 3-OH-B(a)P, **(C)** UGT2A1\_i1 activity against 5-methyl-chrysene-1,2-diol, and **(D)** UGT2A1\_i2 activity against 5-methyl-chrysene-1,2-diol.

**Figure 3. Effect of increasing UGT2A1\_i2 expression on UGT2A1\_i1 glucuronidation activity.** **(A)** Representative Western blot showing stable expression of UGT2A1\_i1\_V5 and induction of UGT2A1\_i2\_FLAG expression in HEK293 cells. UGT2A1\_i2\_FLAG expression was induced through addition of increasing doses of Ponasterone A (PonA) for 12 h; 50  $\mu\text{g}$  of total protein homogenate from each PonA treatment group was loaded per lane for each Western blot. **(B)** A Western blot with 100



JPET #198770

$\mu$ g protein from the control and 10  $\mu$ M PonA treatment groups was performed with an anti-UGT2A1 antibody to confirm UGT2A1 expression levels detected by the anti-V5 and anti-FLAG antibodies. For both panels A and B the relative expression of UGT2A1\_i1, as well as the relative UGT2A1\_i2:UGT2A1\_i1 ratio, was determined for each treatment group. Induction of UGT2A1\_i2 expression and Western blots were performed in triplicate. In all cases,  $\beta$ -actin was used as a loading control. **(C)** Shown are representative chromatograms showing the effect of increasing UGT2A1\_i2 expression on UGT2A1\_i1 activity against 1-OH-pyrene. **(D)** Michaelis-Menten kinetic curves for 1-OH-pyrene, 3-OH B(a)P, and B(a)P-7,8-diol glucuronidation by UGT2A1\_i1, showing the effect of increasing expression levels of UGT2A1\_i2 on UGT2A1\_i1 enzyme activity.

#### **Figure 4. Hetero-oligomerization between UGT2A1\_i1 and UGT2A1\_i2**

**demonstrated by co-IP. (A)** The UGT2A1\_i1\_V5/UGT2A1\_i2\_FLAG complex was immunoprecipitated with an anti-FLAG antibody, then visualized with a HRP-labeled V5 antibody (lane 5). Homogenates from cells over-expressing UGT2A1\_i1\_V5 (lane 1) or UGT2A1\_i2\_FLAG (lane 2) alone were used as negative controls. Dynabeads without antibody conjugation were used as an additional negative control (lane 3). The UGT2A1\_i1\_V5:UGT2A1\_i2\_FLAG complex was immunoprecipitated with an anti-V5 antibody, and then visualized with an anti-V5-HRP antibody as a positive control (lane 4). **(B)** The UGT2A1\_i1\_V5/UGT2A1\_i2\_FLAG complex was immunoprecipitated with an anti-V5 antibody, then visualized with a HRP-labeled FLAG antibody (lane 5). Homogenates from cells over-expressing UGT2A1\_i1\_V5 (lane 1) or UGT2A1\_i2\_FLAG

JPET #198770

(lane 2) alone were used as negative controls. Dynabeads without antibody conjugation were used as an additional negative control (lane 3). The UGT2A1\_i1\_V5:UGT2A1\_i2\_FLAG complex was immunoprecipitated with an anti-FLAG antibody, and then visualized with an anti-FLAG-HRP antibody as a positive control (lane 4). All co-IP experiments were repeated 4-6 times to verify the protein-protein interactions between UGT2A1\_i1 and UGT2A1\_i2.

**Figure 5. Homo-oligomerization of UGT2A1\_i1 demonstrated by co-IP. (A)**

Representative Western blot showing stable expression of UGT2A1\_i1\_V5 and induction of UGT2A1\_i1\_FLAG expression in inducible co-expressed cell line.

UGT2A1\_i1\_FLAG expression was induced through addition of 10  $\mu$ M PonA for 12 h.

50  $\mu$ g of control and PonA treated protein was used for each Western blot, with the ratio of UGT2A1\_i1 to UGT2A1\_i1 expression determined to be approximately 1:1. **(B)** A

Western blot using 100  $\mu$ g protein from the control and 10  $\mu$ M PonA treatment groups was performed using an anti-UGT2A1 antibody to confirm UGT2A1 expression levels detected by the anti-V5 and anti-FLAG antibodies in panel A. **(C)** The

UGT2A1\_i1\_V5/UGT2A1\_i1\_FLAG complex was immunoprecipitated with an anti-FLAG antibody, then visualized with a HRP-labeled V5 antibody (lane 5). Homogenates from cells over-expressing UGT2A1\_i1\_V5 (lane 1) or UGT2A1\_i1\_FLAG (lane 2) alone were used as negative controls. Dynabeads without antibody conjugation were used as an additional negative control (lane 3). The UGT2A1\_i1\_V5:UGT2A1\_i1\_FLAG complex was immunoprecipitated with an anti-V5 antibody, and then visualized with an anti-V5-HRP antibody as a positive control (lane 4). **(D)** The UGT2A1\_i1\_V5/UGT2A1\_i1\_FLAG

JPET #198770

complex was immunoprecipitated with an anti-V5 antibody, then visualized with a HRP-labeled FLAG antibody (lane 5). Homogenates from cells over-expressing UGT2A1\_i1\_V5 (lane 1) or UGT2A1\_i1\_FLAG (lane 2) alone were used as negative controls. Dynabeads without antibody conjugation were used as an additional negative control (lane 3). The UGT2A1\_i1\_V5:UGT2A1\_i1\_FLAG complex was immunoprecipitated with an anti-FLAG antibody, and then visualized with an anti-FLAG-HRP antibody as a positive control (lane 4). All co-IP experiments were repeated 4-6 times to verify UGT2A1\_i1 homo-oligomerization.

**Figure 6. Glucuronidation activity of UGT1A7, UGT1A10, or UGT2B17 against 3-OH-B(a)P and 1-naphthol following co-expression with UGT2A1\_i1 or UGT2A1\_i2.**

**(A)** Real-time PCR was used to determine approximate mRNA levels of each UGT in stable co-expressed HEK293 over-expressing cell lines. ABI gene expression assays were used to quantitatively detect levels of UGT2A1, UGT1A7, UGT1A10, or UGT2B17 transcript. Relative UGT2A1 $\Delta$ exon3 levels were determined by comparing mRNA levels of UGT2A1 $\Delta$ exon3 transcript with UGT1A7, UGT1A10, and UGT2B17 mRNA using the  $\Delta\Delta$ Ct method. Similar experiments were completed to determine wild-type (wt) UGT2A1 mRNA levels relative to UGT1A10 or UGT2B17 levels in additional co-expressed cell lines. Data are expressed as the mean  $\pm$  standard deviation of quadruplicate experiments and were normalized to RPLPO protein levels in each cell line and corrected for differences in assay efficiencies. **(B)** Representative Michaelis-Menten kinetics curves summarizing activity data using homogenates from HEK293 cell lines over-expressing UGT1A7 or UGT1A7 + UGT2A1\_i2 against 3-OH-B(a)P, UGT1A10

JPET #198770

UGT1A10 + UGT2A1\_i2 against 3-OH-B(a)P, and UGT2B17 or UGT2B17 +  
UGT2A1\_i2 against 1-naphthol.

**Table 1.** Kinetic analysis of the effect of UGT2A1\_i2 co-expression on UGT2A1\_i1 activity against PAH substrates.<sup>a</sup>

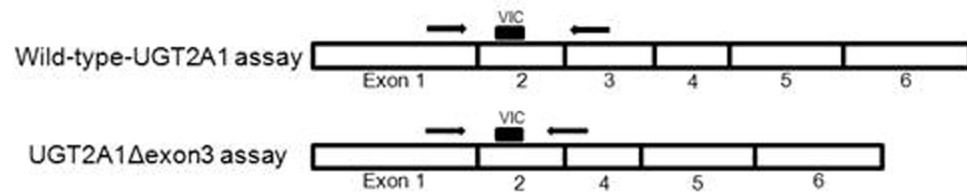
	1-HP			3-OH B(a)P			B(a)P-7,8-diol		
	K <sub>M</sub> ( $\mu$ M)	V <sub>max</sub> (pmol/min/mg)	V <sub>max</sub> /K <sub>M</sub> ( $\mu$ L/min/mg)	K <sub>M</sub> ( $\mu$ M)	V <sub>max</sub> (pmol/min/mg)	V <sub>max</sub> /K <sub>M</sub> ( $\mu$ L/min/mg)	K <sub>M</sub> ( $\mu$ M)	V <sub>max</sub> (pmol/min/mg)	V <sub>max</sub> /K <sub>M</sub> ( $\mu$ L/min/mg)
Vehicle control	159 $\pm$ 16	319 $\pm$ 12 <sup>*</sup>	2.0 $\pm$ 0.08 <sup>*</sup>	256 $\pm$ 32	82 $\pm$ 4.3 <sup>*</sup>	0.32 $\pm$ 0.04 <sup>*</sup>	230 $\pm$ 22	86 $\pm$ 3.6 <sup>*</sup>	0.37 $\pm$ 0.04 <sup>*</sup>
2 $\mu$ M PonA	140 $\pm$ 16	261 $\pm$ 11	1.9 $\pm$ 0.09	276 $\pm$ 20	74 $\pm$ 2.2	0.27 $\pm$ 0.02	253 $\pm$ 37	70 $\pm$ 4.6	0.28 $\pm$ 0.05
6 $\mu$ M PonA	145 $\pm$ 17	219 $\pm$ 8.8	1.5 $\pm$ 0.1	261 $\pm$ 24	64 $\pm$ 2.4	0.24 $\pm$ 0.005	224 $\pm$ 19	53 $\pm$ 2.0	0.24 $\pm$ 0.02
10 $\mu$ M PonA	138 $\pm$ 12	153 $\pm$ 5.6	1.1 $\pm$ 0.08	238 $\pm$ 24	47 $\pm$ 1.9	0.20 $\pm$ 0.01	205 $\pm$ 32	41 $\pm$ 2.6	0.20 $\pm$ 0.01

<sup>a</sup> Data expressed as mg of total protein homogenate, corrected for relative UGT2A1\_i1 expression. K<sub>M</sub> and V<sub>max</sub> represent the mean of three independent experiments.

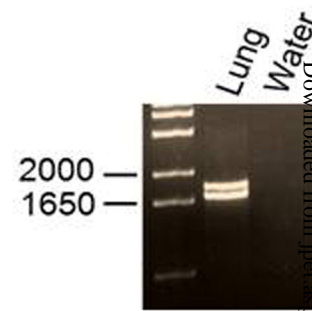
<sup>\*</sup>  $p_{(\text{trend})} < 0.01$ .

**Figure 1**

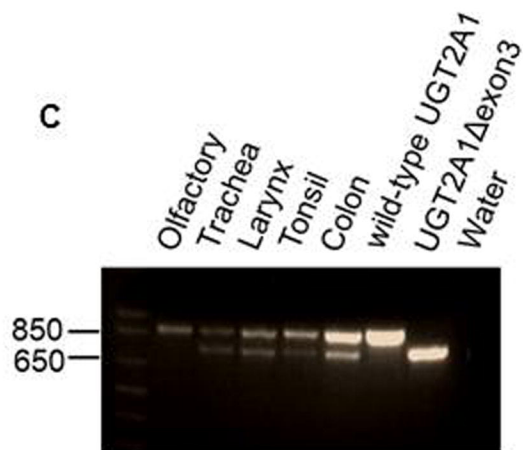
**A**



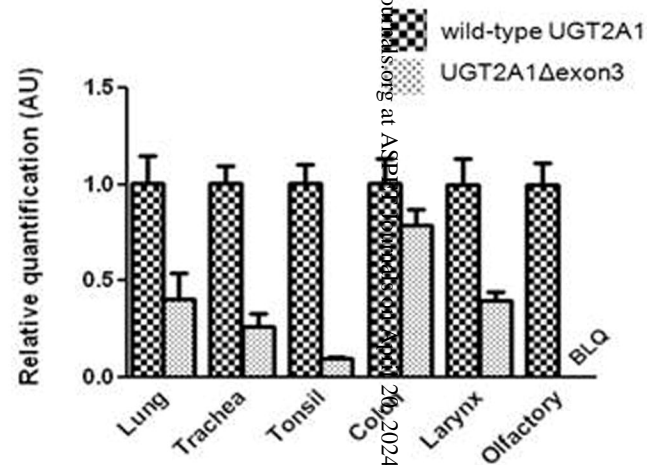
**B**



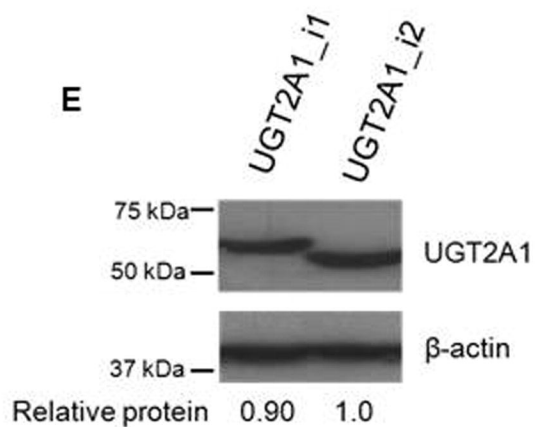
**C**



**D**



**E**



**F**

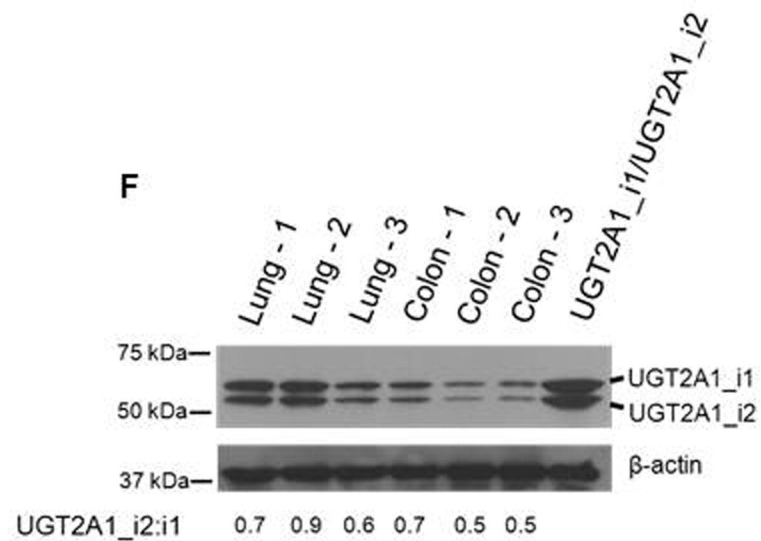
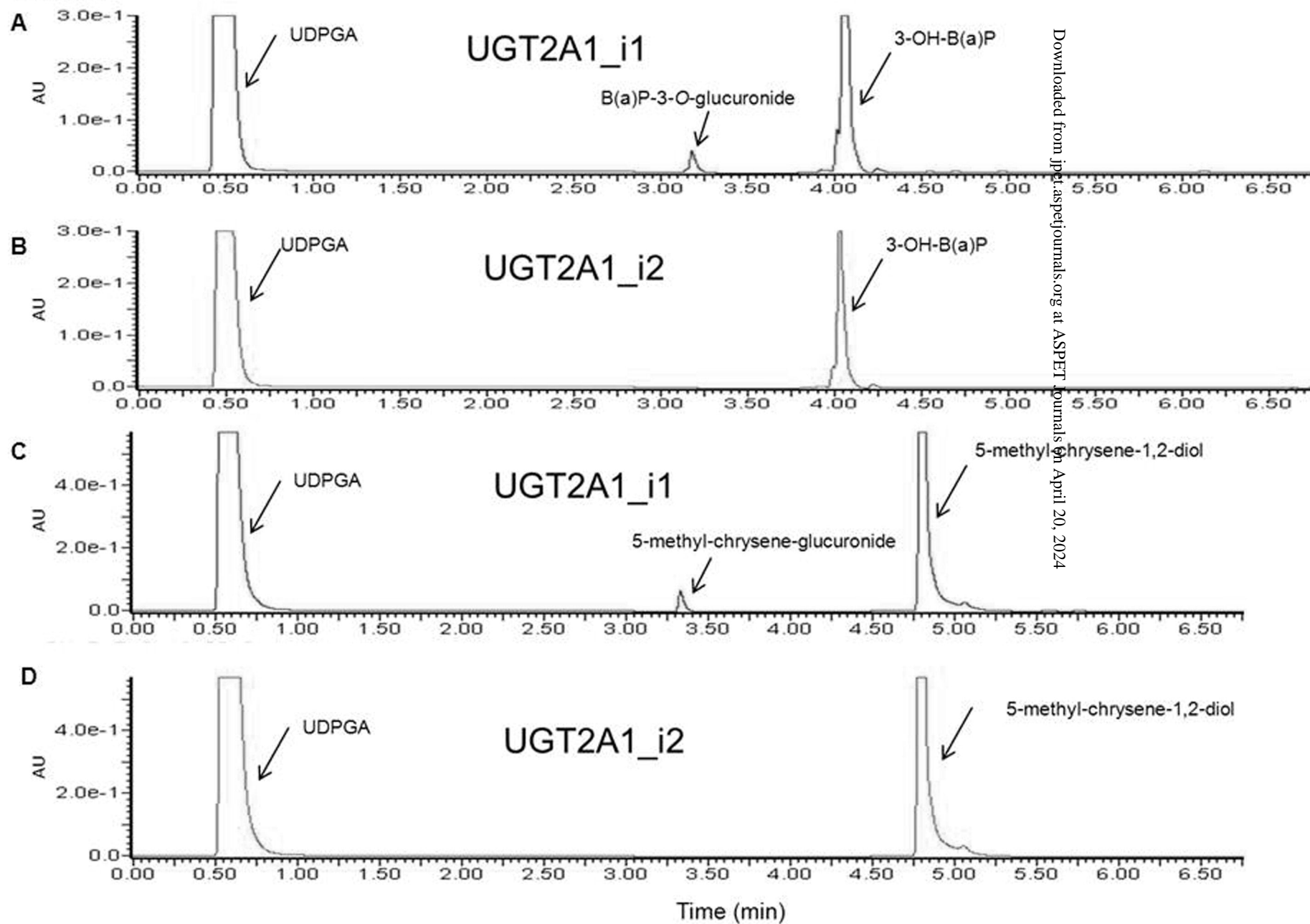
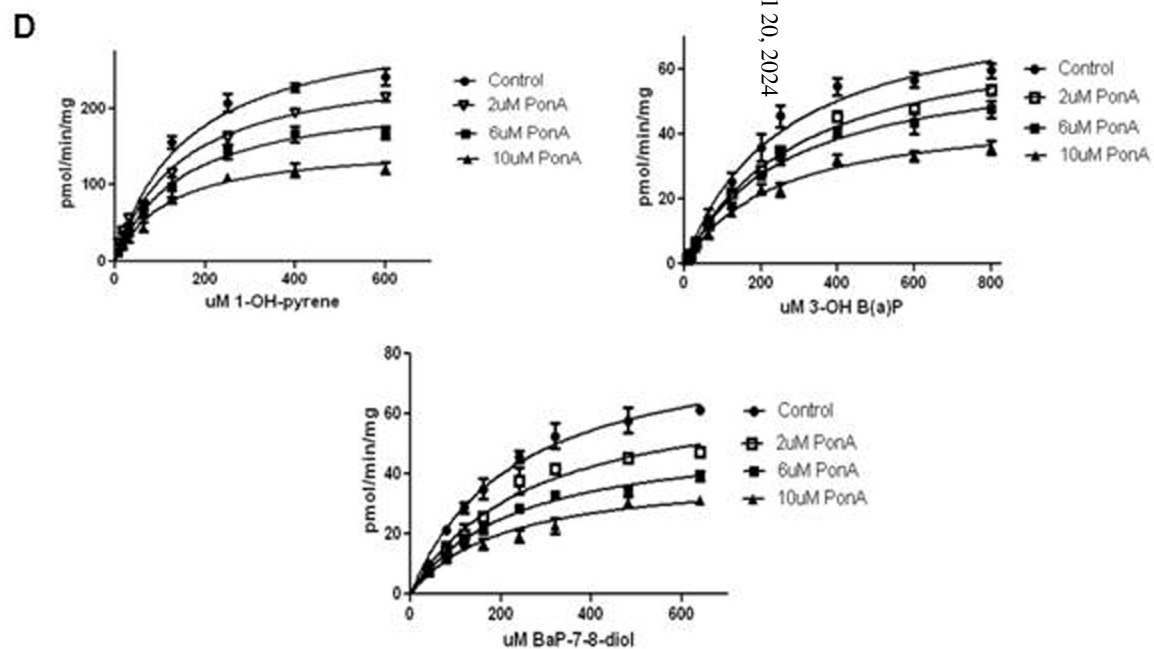
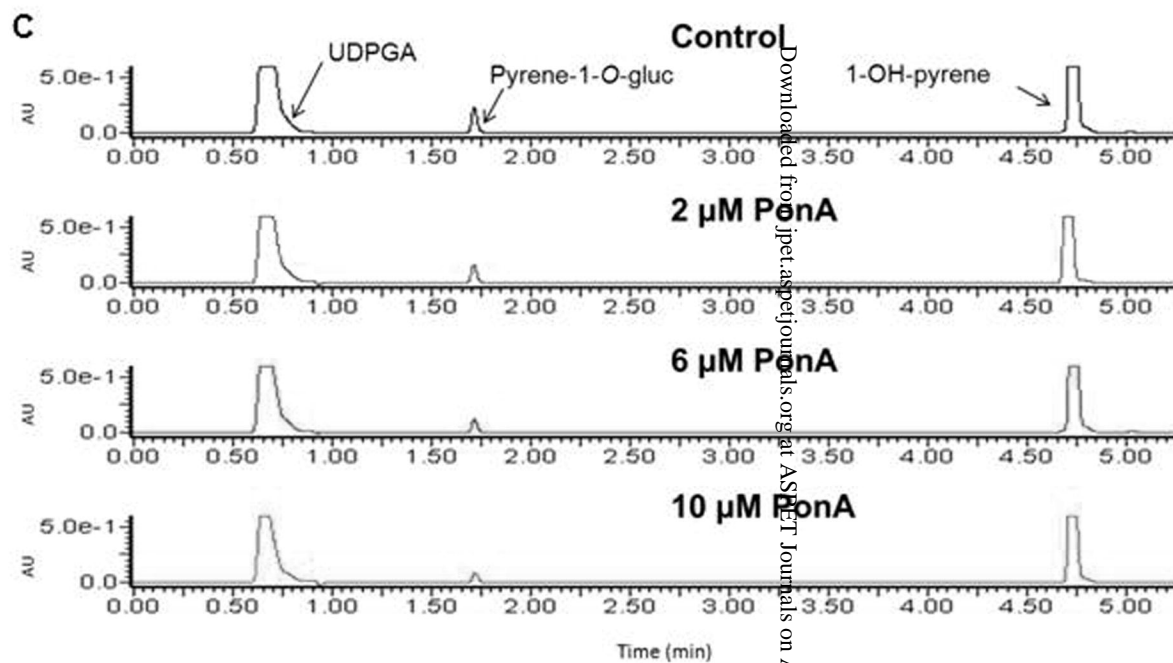
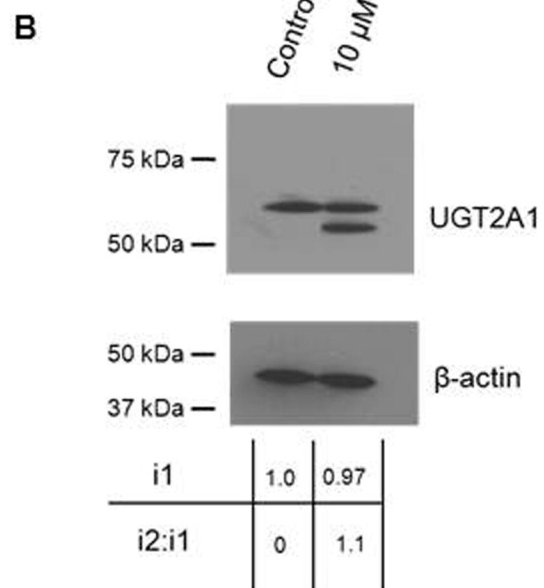
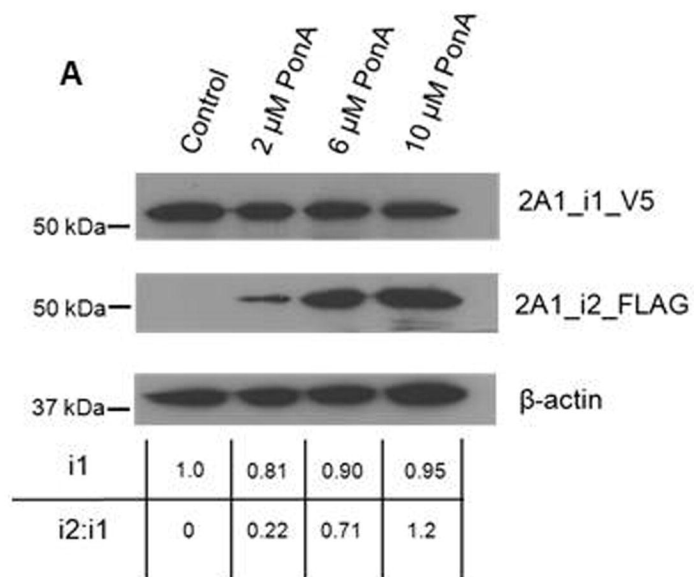


Figure 2



**Figure 3**

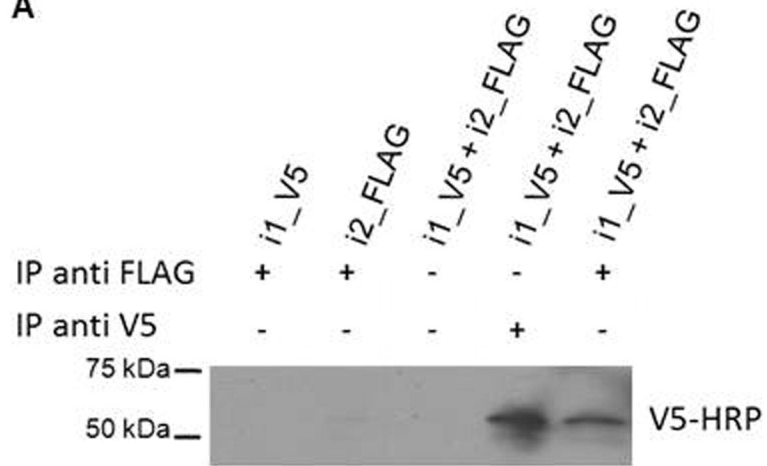


Downloaded from ipet.aspenjournals.org at ASSET Journals on April 20, 2024



Figure 4

**A**



**B**

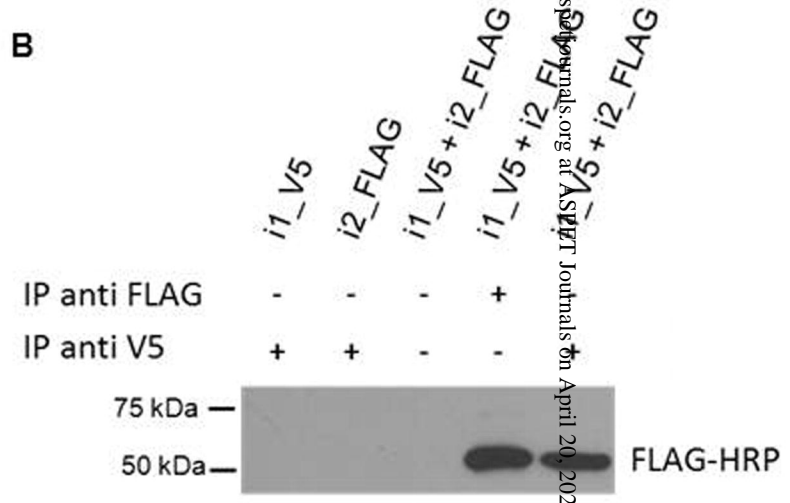
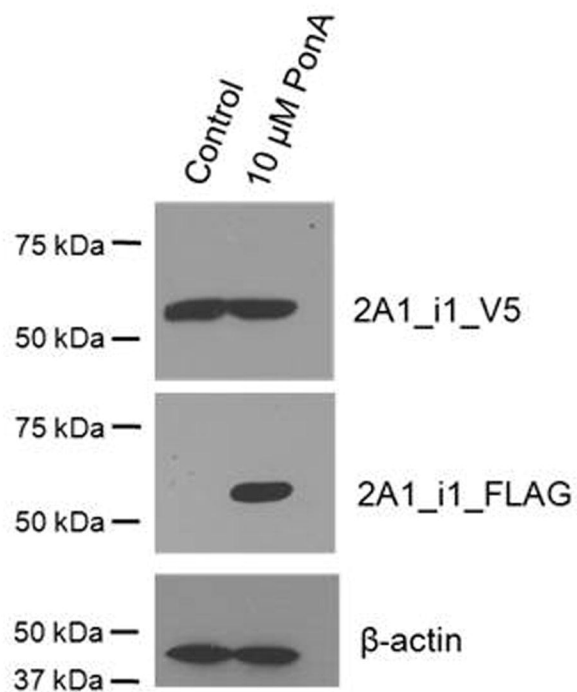
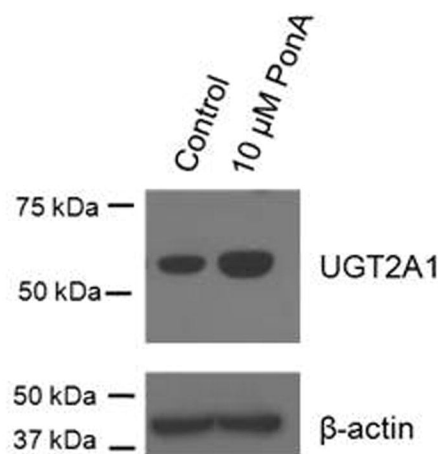


Figure 5

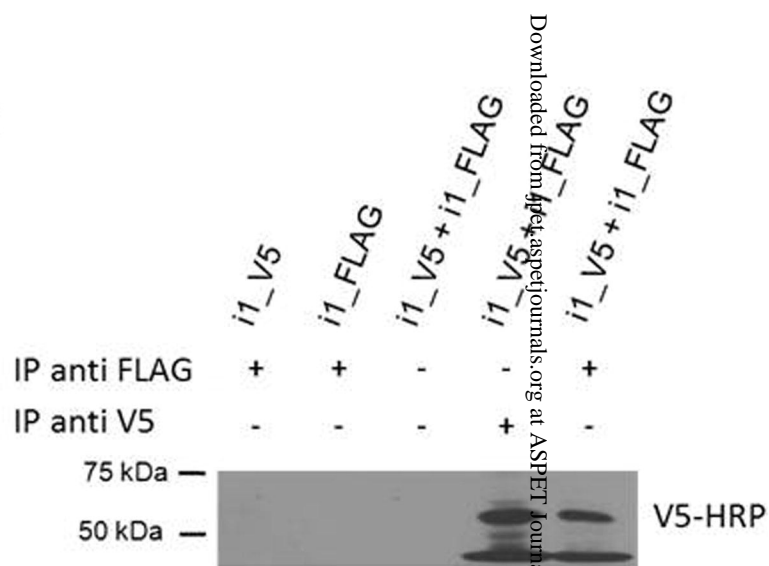
A



B



C



D

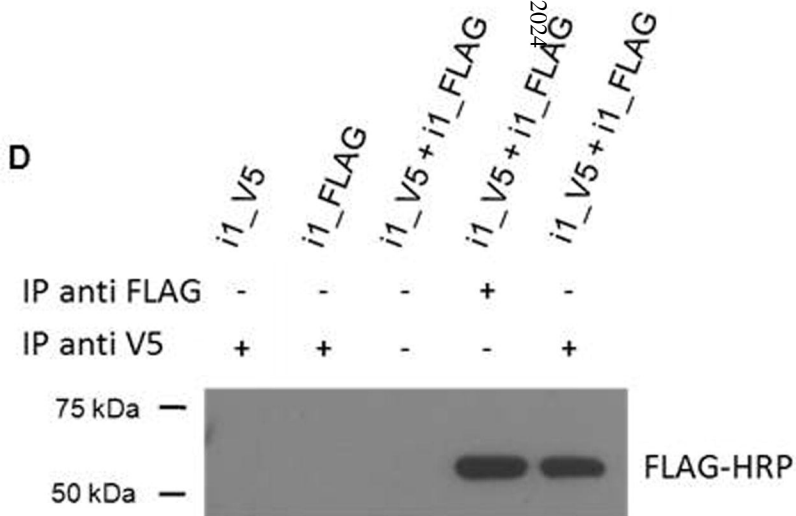
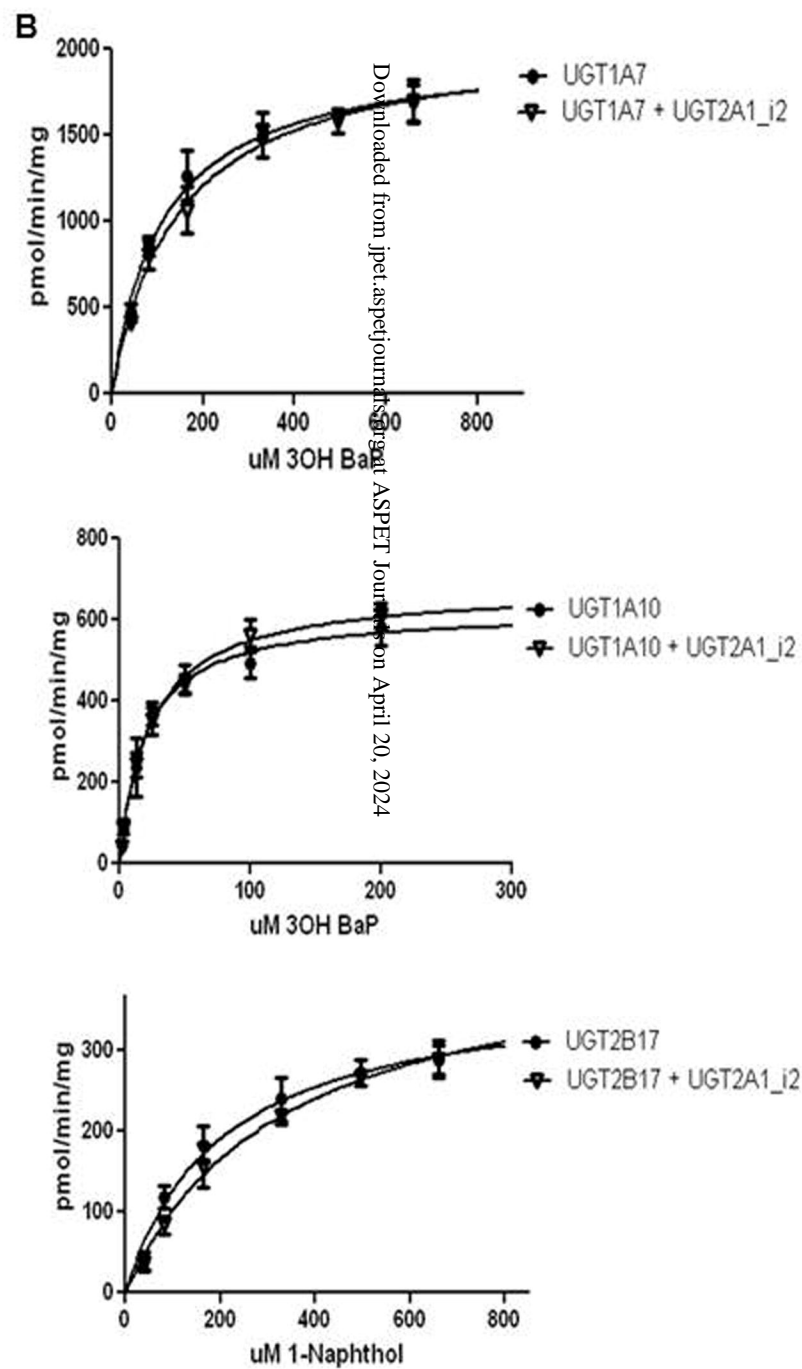
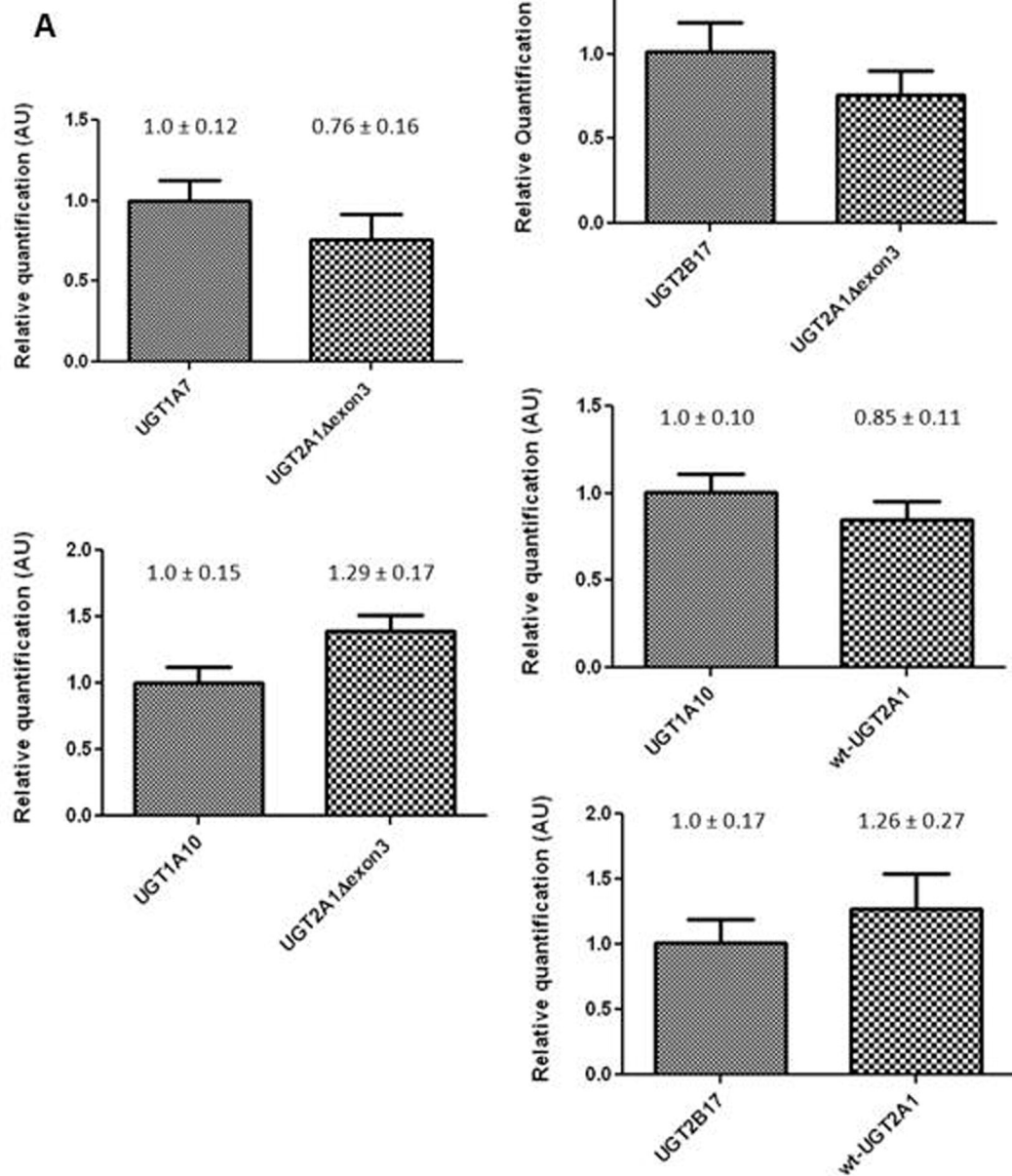


Figure 6



Ryan T. Bushey and Philip Lazarus

**Identification and functional characterization of a novel UGT2A1 splice variant: Potential importance in tobacco-related cancer susceptibility**

**Supplemental Materials and Methods**

*Generation of a UGT2A1<sub>i2</sub> over-expressing cell line and UGT2A1<sub>i2</sub> cell*

*homogenate.* UGT2A1<sub>exonΔ3</sub> was cloned from pooled lung RNA using *Pfu* Polymerase and the UGT2A1\_S1 and UGT2A1\_AS1 primers. Following gel extraction and sequencing of the PCR product of the appropriate size, the verified UGT2A1<sub>exonΔ3</sub> cDNA was cloned into the pcDNA 3.1/V5-His-TOPO vector using standard protocols and grown in One Shot TOP10 competent E.Coli. After direct dideoxy sequencing for sequence confirmation and a large-scale plasmid preparation, electroporation (200 V, 1000 μF) with 10 μg of the pcDNA 3.1/V5-His-TOPO\_UGT2A1<sub>exonΔ3</sub> vector was used to generate the HEK293 cell line over-expressing UGT2A1<sub>i2</sub>. Cells were grown in DMEM supplemented with 10% FBS, 1% penicillin-streptomycin, and 400 μg/mL G418 to 75% confluence. Cell homogenates were prepared essentially as previously described in 1X Tris-buffered saline (25 mM Tris base, 138 mM NaCl and 2.7 mM KCl; pH 7.4) (Dellinger et al., 2006; Sun et al., 2006). Total RNA was extracted using the RNeasy Mini kit using the manufacturer's protocols. Homogenate protein concentrations were determined using the BCA protein assay.

*Determination of UGT2A1<sub>i1</sub> homo-oligomerization.* An inducible co-expression system, similar to that used to investigate UGT2A1<sub>1</sub>:UGT2A1<sub>i2</sub> hetero-oligomerization, was used to examine potential UGT2A1<sub>i1</sub> homo-oligomerization.

Creation of the pcDNA 6.2/V5/GW/D-TOPO\_wtUGT2A1 vector was described previously in the Materials and Methods. Wild-type UGT2A1 was cloned into the FLAG tagged, hygromycin resistance containing pEGSH vector, using UGT2A1\_S3 and UGT2A1\_AS3 primers as described previously. A HEK293 cell line stably expressing the pcDNA6.2/V5/GW/D-TOPO\_wtUGT2A1, pEGSH\_wtUGT2A1, and pERV vectors was created as described in the Materials and Methods. UGT2A1\_i1\_FLAG expression was induced by treating HEK293 cells at 50% confluence with 10  $\mu$ M of PonA (in ethanol) for 12 h. Vehicle (0.01% ethanol) was added to HEK293 cells as a negative control. Determination of UGT2A1\_i1\_V5 and UGT2A1\_i1\_FLAG expression levels using the anti-V5 and anti-FLAG antibodies, the use of the anti-UGT2A1 antibody to confirm UGT2A1\_i1\_V5 and UGT2A1\_i1\_FLAG levels, and co-IP experiments were completed using identical conditions to that described for UGT2A1\_i1\_V5 and UGT2A1\_i2\_FLAG hetero-oligomerization.